

No. 479

Joachim Grammig, Eva-Maria Schaub

## Give me strong moments and time: Combining GMM and SMM to estimate long-run risk asset pricing models

## The CFS Working Paper Series

presents ongoing research on selected topics in the fields of money, banking and finance. The papers are circulated to encourage discussion and comment. Any opinions expressed in CFS Working Papers are those of the author(s) and not of the CFS.

The Center for Financial Studies, located in Goethe University Frankfurt's House of Finance, conducts independent and internationally oriented research in important areas of Finance. It serves as a forum for dialogue between academia, policy-making institutions and the financial industry. It offers a platform for top-level fundamental research as well as applied research relevant for the financial sector in Europe. CFS is funded by the non-profit-organization Gesellschaft für Kapitalmarktforschung e.V. (GfK). Established in 1967 and closely affiliated with the University of Frankfurt, it provides a strong link between the financial community and academia. GfK members comprise major players in Germany's financial industry. The funding institutions do not give prior review to CFS publications, nor do they necessarily share the views expressed therein.

# Give me strong moments and time: Combining GMM and SMM to estimate long-run risk asset pricing models \*

Joachim Grammig and Eva-Maria Schaub \*\*

July 22, 2014

## Abstract

The long-run consumption risk (LRR) model is a promising approach to resolve prominent asset pricing puzzles. The simulated method of moments (SMM) provides a natural framework to estimate its deep parameters, but caveats concern model solubility and weak identification. We propose a two-step estimation strategy that combines GMM and SMM, and for which we elicit informative macroeconomic and financial moment matches from the LRR model structure. In particular, we exploit the persistent serial correlation of consumption and dividend growth and the equilibrium conditions for market return and risk-free rate, as well as the model-implied predictability of the risk-free rate. We match analytical moments when possible and simulated moments when necessary and determine the crucial factors required for both identification and reasonable estimation precision. A simulation study—the first in the context of long-run risk modeling—delineates the pitfalls associated with SMM estimation of a non-linear dynamic asset pricing model. Our study provides a blueprint for successful estimation of the LRR model.

*Key words:* asset pricing, long-run risk, simulated method of moments

*JEL:* C58, G10, G12

---

\*We are grateful to H. Hasseltoft for sharing his MATLAB code for the computation of the endogenous LRR parameters and to J. Krause for providing a MATLAB implementation of the CMAES algorithm. We retain the responsibility for all remaining errors.

\*\*Joachim Grammig: University of Tübingen and Centre for Financial Research (CFR), Cologne, Germany. Address: University of Tübingen, School of Business and Economics, Mohlstrasse 36, D-72074 Tübingen, Germany. [joachim.grammig@uni-tuebingen.de](mailto:joachim.grammig@uni-tuebingen.de), +49-7071-2976009. Eva-Maria Schaub: University of Tübingen. [eva-maria.schaub@uni-tuebingen.de](mailto:eva-maria.schaub@uni-tuebingen.de)

# 1 Introduction

[Bansal and Yaron \(2004\)](#) suggest a dynamic asset pricing model (DAPM) to resolve prominent asset pricing puzzles by accounting for three risk factors: long-run consumption risk, short-run risk, and volatility risk. With its far-reaching impact on model dynamics, the first factor provides the name for the long-run risk (LRR) model. The LRR approach is theoretically appealing, but empirical tests are impeded by an intricate model structure that involves unobserved state variables. As [Singleton \(2006\)](#) points out, the simulated method of moments (SMM) should provide a convenient framework to estimate and test such a complex DAPM.

With this study, we show that to be successful, SMM estimation of the LRR model must account for several theoretical and econometric caveats. For that purpose, we propose a two-step estimation strategy that disentangles the moment matches associated with the macroeconomic and financial system variables, and which reflects the recursive LRR model structure. Our moment matches exploit the persistent serial correlation of consumption and dividends and the equilibrium conditions for market return and risk-free rate, as well as the model-implied predictability of the risk-free rate. We show that failing to account for the recursive model structure when setting up moment matches for the estimation can lead to unreliable results. In a simulation study we delineate the pitfalls associated with the SMM estimation of the LRR model, and we present a blueprint for successful estimation.

Previous empirical assessments of LRR models use both calibration and econometric estimation techniques. [Bansal and Yaron's \(2004\)](#) calibration exercise demonstrates the ability of the LRR model to explain the equity premium. [Bansal et al. \(2007a\)](#) estimate a cointegrated version of the LRR model using a vector autoregressive model with stochastic volatility (SV). However, the LRR model structure

must be adjusted to permit the application of the estimation technique. [Bansal et al. \(2007b\)](#) show that the LRR approach can account for size and value premia in the cross-section. With their calibration of the LRR model, [Drechsler and Yaron \(2011\)](#) explain the variance premium and its relationship to investor preferences. [Bansal and Shaliastovich \(2013\)](#) advocate the LRR approach as a solution to the bond return predictability puzzle. For that purpose, they extend the base model with an inflation process; additional complexity is introduced by two independent SV processes. [Hasseltoft \(2012\)](#) also includes inflation into the LRR framework to model stock and bond markets jointly. [Constantinides and Ghosh \(2011\)](#) make use of the possibility to express the latent model variables as functions of observables, which in turn permits the use of the generalized method of moments (GMM). [Ferson et al. \(2013\)](#) evaluate out-of-sample forecasts produced by a cointegrated version of the LRR model and find the performance to be superior to the stationary model. However, they also impose restrictions to identify some structural parameters from the reduced-form estimates, which is sufficient for forecasting but not for estimating all deep parameters. [Pakoš \(2013\)](#) generalizes the LRR model by introducing incomplete information and a cyclical risk component in the dividend growth rate.

Although the SMM approach to estimating LRR models is natural and appealing, its concrete implementation is impeded by both methodological and numerical intricacies. Such obstacles have largely been ignored—or circumvented—in the previous literature, which is surprising, because it is well known that LRR models are inherently fragile: the permissible parameter space—the set of parameters for which the model has a solution—has a complex topology. For certain economically plausible parameter values, the LRR model becomes insoluble, and the SMM procedure must account for that. Moreover, dividends and consumption are driven by a small but persistent latent growth component and stochastic volatility, which exacerbates

the identification of the structural parameters, especially when the data series are short. The estimation of univariate SV processes has preoccupied researchers for some time.<sup>1</sup> In the LRR model, the SV process is just one element of a complex, non-linear system. It seems daunting to estimate such a model, and we show that it is indeed a losing game to try to estimate the LRR parameters in one step by GMM or SMM using an ad hoc choice of first and second moment matches. Applied researchers may be misled, because weak or non-identification is not always obvious in such a highly non-linear model. It might go unnoticed that even sophisticated optimizers converge to one of the many local minima on the rugged objective function surface.

Our study shows that identification crucially hinges on well-thought moment matches, which must be tailored to the model. We advocate a two-step approach, in which we estimate the subset of parameters associated with the macroeconomic environment separately from the representative investor's preference parameters. The first step consists of a GMM estimation that uses analytical moment conditions resulting from the macro sub-model; the second step is an SMM estimation that exploits asset pricing and predictive relationships implied by the LRR model. We show that the precision of the macro parameter estimates is of utmost importance for the successful estimation of the model parameters. A comprehensive simulation study documents the performance of our estimation strategy. Our findings constitute a call for econometric due diligence and reality checks when estimating a complex DAPM like the LRR model. We also point out that because the available (macro) time series are relatively short, the estimation precision for some of the model parameters will inevitably be limited, emphasizing even more the need for informative

---

<sup>1</sup>Cf. [Ruiz \(1994\)](#), [Gallant et al. \(1997\)](#), [Sandmann and Koopman \(1998\)](#), [Kim et al. \(1998\)](#), [Andersen et al. \(1999\)](#), and [Jacquier et al. \(2002\)](#).

moment matches. The caveats and solutions presented in this study are potentially important for the estimation of other DAPMs as well.

The remainder of the paper is organized as follows. In Section 2 we review the anatomy of the LRR model, the knowledge of which is necessary to understand the moment matching we propose. Section 3 delineates our econometric methodology. In Section 4 we present the results of a Monte Carlo simulation study that assesses the suitability of our approach. We conclude in Section 5.

## 2 LRR model anatomy

In this section, we describe the anatomy of the long-run risk model by [Bansal and Yaron \(2004\)](#). We present all key equations needed for the simulation of the model,<sup>2</sup> as well as the intricacies of the model structure that complicate the estimation of its parameters.

### 2.1 Macroeconomy of the LRR model

The LRR model is based on a non-linear, four-equation macro VAR with two observable variables, log consumption growth  $g_t$  and log dividend growth  $g_{d,t}$ , and two latent variables, a growth component  $x_t$  and a stochastic variance process  $\sigma_t^2$ :

$$g_{t+1} = \mu_c + x_t + \sigma_t \eta_{t+1} \tag{1}$$

$$x_{t+1} = \rho x_t + \varphi_e \sigma_t e_{t+1} \tag{2}$$

$$g_{d,t+1} = \mu_d + \phi x_t + \varphi_d \sigma_t u_{t+1} \tag{3}$$

$$\sigma_{t+1}^2 = \sigma^2 + \nu_1(\sigma_t^2 - \sigma^2) + \sigma_w w_{t+1}. \tag{4}$$

---

<sup>2</sup>Detailed derivations are available in Sections A.1–A.5 of the Internet appendix, which can be downloaded from <http://tinyurl.com/lrr-internet-appendix>. These results appear somewhat dispersed in prior literature, so we collect them to provide the interested reader with a complete picture.

The i.i.d. innovations  $\eta_t$ ,  $e_t$ ,  $w_t$ , and  $u_t$ , are standard normally distributed, and contemporaneously uncorrelated random variables. The latent drivers of the economic dynamics  $x_t$  and  $\sigma_t^2$  are assumed to be highly persistent, so the autoregressive parameters  $\rho$  and  $\nu_1$  are usually chosen to be close to 1 in calibration exercises (cf. [Bansal and Yaron, 2004](#)). For a model simulation, the trajectories of  $g_t$ ,  $x_t$ ,  $g_{d,t}$ , and  $\sigma_t^2$  represent the elementary components for all other model variables. Let us collect the parameters of the LRR macroeconomy in the vector  $\xi_M = (\mu_c, \mu_d, \rho, \sigma, \varphi_e, \phi, \varphi_d, \nu_1, \sigma_w)'$ .

## 2.2 Asset pricing with long run risk and model solubility

The representative investor who faces these macro dynamics has recursive preferences (cf. [Epstein and Zin, 1989](#)), as expressed by the utility function

$$U_t = \left[ (1 - \delta) C_t^{\frac{1-\gamma}{\theta}} + \delta \left( \mathbb{E}_t \left( U_{t+1}^{1-\gamma} \right) \right)^{\frac{1}{\theta}} \right]^{\frac{\theta}{1-\gamma}}, \quad (5)$$

where  $\theta = \frac{(1-\gamma)}{(1-\frac{1}{\psi})}$ . The preference parameters  $\delta$ ,  $\gamma$ , and  $\psi$  denote the subjective discount factor, relative risk aversion, and intertemporal elasticity of substitution (IES), respectively. Let us collect the preference parameters in the vector  $\xi_P = (\delta, \gamma, \psi)'$ . The representative investor has aggregate wealth  $W_t$  and consumption  $C_t$ . Utility maximization under the budget constraint  $W_{t+1} = (W_t - C_t)R_{a,t+1}$ , where  $R_{a,t}$  denotes the gross return of the latent aggregate wealth portfolio, yields the basic asset pricing equation for a gross asset return  $R_{i,t}$ :

$$\mathbb{E}_t [M_{t+1} R_{i,t+1} - 1] = 0, \quad (6)$$

where

$$M_{t+1} = \delta^\theta G_{t+1}^{-\frac{\theta}{\psi}} R_{a,t+1}^{-(1-\theta)} \quad (7)$$



denotes the stochastic discount factor (SDF), and  $G_t$  denotes gross consumption growth.

[Bansal and Yaron \(2004\)](#) explicitly model the log returns of the latent aggregate wealth portfolio and the observable market portfolio,  $r_{a,t}$  and  $r_{m,t}$ , using the linear approximations suggested by [Campbell and Shiller \(1988\)](#):<sup>3</sup>

$$r_{a,t+1} = \kappa_0 + \kappa_1 z_{t+1} - z_t + g_{t+1} \quad (8)$$

$$r_{m,t+1} = \kappa_{0,m} + \kappa_{1,m} z_{m,t+1} - z_{m,t} + g_{d,t+1}, \quad (9)$$

where  $z_t$  denotes the log price-consumption ratio, and  $z_{m,t}$  is the log price-dividend ratio. Furthermore,

$$\kappa_1 = \frac{\exp(\bar{z})}{1 + \exp(\bar{z})} \quad \kappa_{1,m} = \frac{\exp(\bar{z}_m)}{1 + \exp(\bar{z}_m)} \quad (10)$$

$$\kappa_0 = \ln(1 + \exp(\bar{z})) - \kappa_1 \bar{z} \quad \kappa_{0,m} = \ln(1 + \exp(\bar{z}_m)) - \kappa_{1,m} \bar{z}_m, \quad (11)$$

where  $\bar{z}$  and  $\bar{z}_m$  denote the means of  $z_t$  and  $z_{m,t}$ . [Bansal and Yaron \(2004\)](#) model the latent log price-consumption ratio and the observable log price-dividend ratio as

$$z_t = A_0 + A_1 x_t + A_2 \sigma_t^2 \quad (12)$$

$$z_{m,t} = A_{0,m} + A_{1,m} x_t + A_{2,m} \sigma_t^2. \quad (13)$$

The parameters in Equations (12) and (13) must be determined by an analytical solution of the model (details in the Internet appendix). The solution is obtained by

---

<sup>3</sup>Detailed derivations of Equations (8)–(11) are in Section A.1 of the Internet appendix.

pricing the gross returns of the aggregate wealth portfolio and the market portfolio,  $R_{a,t}$  and  $R_{m,t}$ , using Equation (6), which yields:

$$A_1 = \frac{1 - \frac{1}{\psi}}{1 - \kappa_1 \rho} \quad (14)$$

$$A_2 = \frac{1 \left( \theta - \frac{\theta}{\psi} \right)^2 + (\theta A_1 \kappa_1 \varphi_e)^2}{2 \theta (1 - \kappa_1 \nu_1)} \quad (15)$$

$$A_0 = \frac{1}{1 - \kappa_1} \left[ \ln \delta + \left( 1 - \frac{1}{\psi} \right) \mu_c + \kappa_0 + \kappa_1 A_2 \sigma^2 (1 - \nu_1) + \frac{\theta}{2} (\kappa_1 A_2 \sigma_w)^2 \right] \quad (16)$$

$$A_{1,m} = \frac{\phi - \frac{1}{\psi}}{1 - \kappa_{1,m} \rho} \quad (17)$$

$$A_{2,m} = \frac{(1 - \theta)(1 - \kappa_1 \nu_1) A_2}{(1 - \kappa_{1,m} \nu_1)} + \frac{\frac{1}{2} \left[ \left( -\frac{\theta}{\psi} + \theta - 1 \right)^2 + ((\kappa_{1,m} A_{1,m} \varphi_e) - ((1 - \theta) \kappa_1 A_1 \varphi_e))^2 + \varphi_d^2 \right]}{(1 - \kappa_{1,m} \nu_1)} \quad (18)$$

$$A_{0,m} = \frac{1}{(1 - \kappa_{1,m})} \left[ \theta \ln \delta - \frac{\theta}{\psi} \mu_c + (\theta - 1) \left[ \kappa_0 + \kappa_1 A_0 + \kappa_1 A_2 (1 - \nu_1) \sigma^2 - A_0 + \mu_c \right] + \kappa_{0,m} + \kappa_{1,m} A_{2,m} \sigma^2 (1 - \nu_1) + \mu_d + \frac{1}{2} [(\theta - 1) \kappa_1 A_2 + \kappa_{1,m} A_{2,m}]^2 \sigma_w^2 \right] \quad (19)$$

The  $A$ -parameters given by Equations (14)–(19) depend on  $\kappa_0$ ,  $\kappa_1$ ,  $\kappa_{0,m}$ , and  $\kappa_{1,m}$  from Equations (10) and (11), which in turn depend on  $\bar{z}$  and  $\bar{z}_m$ . As a consequence, the  $\kappa$ -parameters, and thus the  $A$ -parameters, are endogenous.

To estimate the LRR model by SMM, we need to generate series of  $z_t$ ,  $z_{m,t}$ ,  $r_{a,t}$ , and  $r_{m,t}$ . For that purpose we must solve the model, i.e. find  $\bar{z}$  and  $\bar{z}_m$  such that Equations (10)–(19) are fulfilled. This is achieved by solving for the mean of  $z_t$  and  $z_{m,t}$ , such that the squared difference between the respective mean hypothesized by the solver and the resulting model-implied mean is equal to zero. Hence, the endogenous parameters are implied by the roots of two functions.

[Insert Figure 1 about here]

Figure 1 illustrates that this structure makes the LRR model inherently fragile. The upper panels show a plot of these two functions and their roots, based on the LRR parameter values chosen by [Bansal and Yaron \(2004\)](#) for their calibration of the LRR model (see Table 2). The lower panels show that a change of these parameters within a plausible range can yield an unsolvable model. This fragility of the LRR model thus exacerbates parameter estimation.

As we outline below, our estimation approach exploits the implications of the LRR model for the log risk-free rate  $r_{f,t}$ . To obtain the LRR model-implied expression for  $r_{f,t}$ , we price a risk-free payoff using Equation (6), which yields:

$$r_{f,t} = -\theta \ln(\delta) + \frac{\theta}{\psi} [\mu_c + x_t] + (1 - \theta) \mathbb{E}_t(r_{a,t+1}) - \frac{1}{2} \text{Var}_t(m_{t+1}), \quad (20)$$

where  $m_t$  is the logarithm of the stochastic discount factor  $M_t$  and

$$\begin{aligned} \mathbb{E}_t(r_{a,t+1}) &= \kappa_0 + \kappa_1 [A_0 + A_1 \rho x_t + A_2(\sigma^2 + \nu_1(\sigma_t^2 - \sigma^2))] \\ &\quad - A_0 - A_1 x_t - A_2 \sigma_t^2 + \mu_c + x_t, \end{aligned} \quad (21)$$

$$\begin{aligned} \text{Var}_t(m_{t+1}) &= \left( \frac{\theta}{\psi} + 1 - \theta \right)^2 \sigma_t^2 + [(1 - \theta) \kappa_1 A_1 \varphi_e]^2 \sigma_t^2 \\ &\quad + [(1 - \theta) \kappa_1 A_2]^2 \sigma_w^2. \end{aligned} \quad (22)$$

The derivation of Equations (20)–(22) can be found in Section A.4 of the Internet appendix.

### 3 Econometric methodology

#### 3.1 Matching moments for the LRR model: choices and caveats

Singleton (2006) suggests using the simulated method of moments to estimate non-linear dynamic asset pricing models like the LRR model, arguing that the method is well suited to dealing with non-linearity, latent variables, and endogenous model parameters—those complexity-driving features of the LRR model. To apply GMM, we have to select a vector of measurable functions  $\mathbf{g}(\mathbf{q}_t; \boldsymbol{\xi})$ , where  $\mathbf{q}_t$  contains the macroeconomic and financial system variables, and  $\boldsymbol{\xi} = (\boldsymbol{\xi}'_M, \boldsymbol{\xi}'_P)'$ , and derive the model-implied expectations. Observations of  $\mathbf{g}(\cdot)$  are collected in the vector  $\mathbf{g}_t^*$ . A match of sample moments with theoretical moments yields:

$$\mathbf{G}_T(\boldsymbol{\xi}) = \frac{1}{T} \sum_{t=1}^T \mathbf{g}_t^* - \mathbb{E}[\mathbf{g}(\mathbf{q}_t; \boldsymbol{\xi})], \quad (23)$$

where  $T$  denotes the sample size. SMM is applied when the population moments cannot be expressed analytically as functions of  $\boldsymbol{\xi}$  but must be simulated, such that the moment matches read:

$$\mathbf{G}_T(\boldsymbol{\xi}) = \frac{1}{T} \sum_{t=1}^T \mathbf{g}_t^* - \frac{1}{\mathcal{T}(T)} \sum_{s=1}^{\mathcal{T}(T)} \mathbf{g}(\mathbf{q}_s; \boldsymbol{\xi}), \quad (24)$$

where  $\mathcal{T}(T)$  denotes the simulated sample size. To obtain  $\mathbf{q}_s$  for  $s = 1, \dots, \mathcal{T}(T)$ , we simulate the LRR model using the equations and results outlined in the previous section. A large  $\mathcal{T}(T)$  ensures a good approximation to population moments. GMM estimates, using Equation (23), or SMM estimates, using Equation (24), are obtained from

$$\hat{\boldsymbol{\xi}}_T = \underset{\boldsymbol{\xi} \in \Theta}{\operatorname{argmin}} \mathbf{G}_T(\boldsymbol{\xi})' \mathbf{W}_T \mathbf{G}_T(\boldsymbol{\xi}), \quad (25)$$

where  $\mathbf{W}_T$  is a symmetric and positive definite matrix.

Because the LRR model is a complex, highly non-linear model, it is an appealing idea to estimate its parameters by matching some selected first and second moments of the macro and financial system variables. However, the identification of the deep parameters may require information that is not or is only weakly reflected in the moment matches implied by Equation (25).

This conclusion originates from an attempt to estimate the twelve LRR parameters in  $\boldsymbol{\xi}_M$  and  $\boldsymbol{\xi}_P$  by SMM, using a set of moment matches adapted from [Hasseltoft \(2012\)](#). Panel A of Table 1 shows that the moment matches invoke ten first and second moments of the observable system variables, two autocovariances, as well as two moments based on the prediction relationship between the log price-dividend ratio and squared future shocks to consumption growth.

[Insert Table 1 about here]

[Insert Table 2 about here]

We perform an SMM estimation on simulated data of lengths  $T = 1000$  and  $T = 100,000$ , respectively. These data are generated by an LRR model, for which we use the parameter values of Bansal and Yaron’s (2004) original calibration of the LRR model (cf. Table 2). We use the identity matrix for  $\mathbf{W}_T$  and  $\mathcal{T}(T) = 10^6$ .

Previous studies already hint at numerical difficulties during GMM/SMM estimation of the LRR model, which is reflected in the choice of (global) optimization algorithms.<sup>4</sup> We therefore employ a sophisticated global optimization algorithm, the covariance matrix adaptation evolution strategy (CMAES) developed by [Hansen and Ostermeier \(2001\)](#). We start the optimization of the SMM objective at three

---

<sup>4</sup>[Hasseltoft \(2012\)](#) uses simulated annealing, [Constantinides and Ghosh \(2011\)](#) employ the differential evolution algorithm. These algorithms promise to find the global optimum of rugged objective functions fraught with local minima.

different, but not very dissimilar, vectors of initial values. The initial vector  $\xi_{s_1}$  corresponds to the true parameters, which we slightly change for  $\xi_{s_2}$ . The initial values in  $\xi_{s_3}$  are further away from the true parameters but still perfectly reasonable.

Panel A of Table 3 documents a disturbing result that raises doubts about whether it is possible to estimate the LRR parameters by SMM based on the ad hoc moment matches given in Panel A of Table 1. Using the different initial values, the optimization for simulated data of length  $T = 100,000$  terminates at different parameter values (some vastly different), though they all fulfill the convergence criteria.<sup>5</sup> The conclusion is evident: You can obtain different (convenient) parameter estimates by choosing different starting values. The ad hoc moment matches that invoke the augmented first two moments are valid, but they are not helpful to identify the structural parameters, even in large samples. Using alternative weighting matrices in Equation (25), such as an estimate of the efficient weighting matrix, does not resolve the problem.

[Insert Table 3 about here]

The non-linear LRR model structure precludes an analytic identification check. However, we can provide numerical evidence. Table 4 displays the percentage change of each moment in Panel A of Table 1 in response to a 50% c.p. decrease of one of the LRR model parameters.

[Insert Table 4 about here]

There is very little or no sensitivity of the moments to changes in the SV parameters  $\nu_1$  and  $\sigma_w$ . The largest impact of a 50% decrease of  $\nu_1$  ( $\sigma_w$ ) is a 4% (3%) decrease

---

<sup>5</sup>This problem occurs for all optimization algorithms we applied, inter alia simulated annealing, genetic algorithm, and pattern search from MATLAB's Global Optimization Toolbox. The CMAES used in Panel A of Table 3, which is specifically designed to deal with very rugged objective functions, cannot resolve this issue.

in the mean market excess return. These very weak responses by a moment, which is very sensitive to many other model parameters, make it doubtful that the SV parameters are identified. Considering the previous efforts invested in SV estimation, this caveat does not come as a surprise. Parameter estimation is hampered not only by the presence of stochastic volatility, though. Repeating the estimation procedure without SV in the data generating process delivers the same result: Reliable global optimization is infeasible, even when using sophisticated optimizers.

The GMM-based estimation strategy put forth by [Constantinides and Ghosh \(2011\)](#), which uses the moments in Panel B of Table 1, is prone to the same problem. Panel B of Table 3 shows that the algorithm that minimizes the GMM objective converges to different points when started from alternative initial values, producing the same question: Can the chosen moment matches ensure the identification of the LRR model parameters?

The alarming result of our simulation exercise may also occur for real data: the optimizer stops close to plausibly chosen starting values. If the neighborhood of that point happens to be well-defined, asymptotic inference may yield favorably small standard errors for plausible but utterly arbitrary estimates. A failure of the estimation can be explained by two different scenarios, according to Extremum Estimator theory (cf. e.g. [Singleton, 2006](#)), that cannot be ruled out in the present application. Either, a unique estimator  $\hat{\xi}_T$  does not exist since the limit function of the objective is not uniquely minimized at the true parameter vector, or the estimation fails due to non-compactness of the parameter space.

These starting value dependent results in Table 3 are disturbing as they question the ability of GMM/SMM to deal with the complexity of the LRR model. But we will show that reliable results can be achieved. The key insight is that the moment matches must reflect the recursive structure of the LRR model, and that you need

to incorporate the LRR model characteristics in strong moment matches. We will explain our solutions in the next sections.

### 3.2 Disentangling LRR moment matches

The recursive structure of the LRR model suggests moment matches that involve macro variables only (consumption and dividend growth), and which therefore only depend on  $\boldsymbol{\xi}_M$ . Let us denote those macro moment matches by  $\mathbf{G}_T^M$ . On the other hand, there are moment matches that involve the financial variables (e.g. market return, risk-free rate), and which will, by LRR anatomy, depend on both  $\boldsymbol{\xi}_M$  and  $\boldsymbol{\xi}_P$ . Let us denote those financial moment matches by  $\mathbf{G}_T^P$ .

Both approaches considered in the previous section minimize the GMM/SMM objective function (25), which entails setting linear combinations of  $\mathbf{G}_T^M$  and  $\mathbf{G}_T^P$  to zero. Using  $\mathbf{G}_T(\boldsymbol{\xi}) = (\mathbf{G}_T^M(\boldsymbol{\xi}_M)', \mathbf{G}_T^P(\boldsymbol{\xi}_P, \boldsymbol{\xi}_P)')$  and properly partitioning  $\mathbf{W}_T$ , this can be seen by writing the first order conditions for the GMM/SMM estimation problem as

$$\underbrace{\begin{bmatrix} \frac{\partial \mathbf{G}_T^M(\boldsymbol{\xi}_M)'}{\partial \boldsymbol{\xi}_M} & \frac{\partial \mathbf{G}_T^P(\boldsymbol{\xi}_M, \boldsymbol{\xi}_P)'}{\partial \boldsymbol{\xi}_M} \\ \mathbf{0} & \frac{\partial \mathbf{G}_T^P(\boldsymbol{\xi}_M, \boldsymbol{\xi}_P)'}{\partial \boldsymbol{\xi}_P} \end{bmatrix}}_{\frac{\partial \mathbf{G}_T(\boldsymbol{\xi})'}{\partial \boldsymbol{\xi}}} \times \underbrace{\begin{bmatrix} \mathbf{W}_T^M & \mathbf{W}_T^{12} \\ \mathbf{W}_T^{21} & \mathbf{W}_T^P \end{bmatrix}}_{\mathbf{W}_T} \times \underbrace{\begin{bmatrix} \mathbf{G}_T^M(\boldsymbol{\xi}_M) \\ \mathbf{G}_T^P(\boldsymbol{\xi}_M, \boldsymbol{\xi}_P) \end{bmatrix}}_{\mathbf{G}_T(\boldsymbol{\xi})} \stackrel{!}{=} \mathbf{0}. \quad (26)$$

Equation (26) shows how the GMM algebra intertwines the financial and macro moment matches. The financial moment matches  $\mathbf{G}_T^P$  affect the estimation of the macro parameters  $\boldsymbol{\xi}_M$  and the macro moment matches  $\mathbf{G}_T^M$  interfere in the estimation of the preference parameters  $\boldsymbol{\xi}_P$ . Using a weighting matrix  $\mathbf{W}_T$  with non-zero elements off the main diagonal generates the most complex mix of moment matches,



but macro and financial moment matches remain entangled when using  $\mathbf{W}_T = \mathbf{I}$ .

In this case, Equation (26) becomes

$$\frac{\partial \mathbf{G}_T^M(\boldsymbol{\xi}_M)'}{\partial \boldsymbol{\xi}_M} \mathbf{G}_T^M(\boldsymbol{\xi}_M) + \frac{\partial \mathbf{G}_T^P(\boldsymbol{\xi}_M, \boldsymbol{\xi}_P)'}{\partial \boldsymbol{\xi}_M} \mathbf{G}_T^P(\boldsymbol{\xi}_M, \boldsymbol{\xi}_P) \stackrel{!}{=} \mathbf{0} \quad (27)$$

$$\frac{\partial \mathbf{G}_T^P(\boldsymbol{\xi}_M, \boldsymbol{\xi}_P)'}{\partial \boldsymbol{\xi}_P} \mathbf{G}_T^P(\boldsymbol{\xi}_M, \boldsymbol{\xi}_P) \stackrel{!}{=} \mathbf{0}. \quad (28)$$

Both previously discussed attempts to estimate the LRR parameters are based on the GMM/SMM objective function in (25), and we suspect that the problems reported in Section 3.1 are caused by the interlacement of macro and financial moment matches, which may not be appropriate in case of the LRR model. The financial moment matches  $\mathbf{G}_T^P$  must identify the preference parameters, in particular distinguish the risk aversion from the IES. Why should they have the additional task to help to identify the macro parameters? By minimizing the GMM objective function in Equation (25), the financial moment matches  $\mathbf{G}_T^P$  cannot but interfere with the estimation of the macro parameters.

We argue that macro and financial moment matches have to be disentangled when estimating the LRR parameters. In particular, only linear combinations of the macro moment matches  $\mathbf{G}_T^M$  should be set to zero to estimate  $\boldsymbol{\xi}_M$ . This entails that the term  $\frac{\partial \mathbf{G}_T^P}{\partial \boldsymbol{\xi}_M} \mathbf{G}_T^P$  should not be present in Equation (27). However, there is no positive definite and symmetric weighting matrix  $\mathbf{W}_T$  that could be constructed to accomplish that task. Disentangling macro and financial moment matches is infeasible when parameter estimates result from a minimization of the GMM/SMM objective function in (25).<sup>6</sup>

Our solution is to conceive the estimation of the LRR parameters as a generic GMM problem (cf. Hansen, 1982). By generic GMM we mean that parameter esti-

---

<sup>6</sup>This is why using an efficient weighting matrix estimate for  $\mathbf{W}_T$  does not resolve, but rather aggravates the estimation problems caused by intertwined moment matches.

mates are obtained by setting linear combinations of moment matches to zero, i.e.  $\mathbf{a}_T(\boldsymbol{\xi})\mathbf{G}_T(\boldsymbol{\xi}) \stackrel{!}{=} \mathbf{0}$ , but not necessarily is  $\mathbf{a}_T(\boldsymbol{\xi}) = \frac{\partial \mathbf{G}_T(\boldsymbol{\xi})'}{\partial \boldsymbol{\xi}} \mathbf{W}_T$  as in Equation (26). The desired disentanglement of moment matches can be achieved by estimating  $\boldsymbol{\xi}_M$  and  $\boldsymbol{\xi}_P$  by solving

$$\underbrace{\begin{bmatrix} \frac{\partial \mathbf{G}_T^M(\boldsymbol{\xi}_M)'}{\partial \boldsymbol{\xi}_M} \mathbf{W}_T^M & \mathbf{0} \\ \mathbf{0} & \frac{\partial \mathbf{G}_T^P(\boldsymbol{\xi}_M, \boldsymbol{\xi}_P)'}{\partial \boldsymbol{\xi}_P} \mathbf{W}_T^P \end{bmatrix}}_{\mathbf{a}_T(\boldsymbol{\xi})} \times \begin{bmatrix} \mathbf{G}_T^M(\boldsymbol{\xi}_M) \\ \mathbf{G}_T^P(\boldsymbol{\xi}_M, \boldsymbol{\xi}_P) \end{bmatrix} \stackrel{!}{=} \mathbf{0}, \quad (29)$$

where  $\mathbf{W}_T^M$  and  $\mathbf{W}_T^P$  are symmetric and positive definite. The resulting estimates  $\hat{\boldsymbol{\xi}}_M$  thus obey

$$\left. \frac{\partial \mathbf{G}_T^M(\boldsymbol{\xi}_M)'}{\partial \boldsymbol{\xi}_M} \right|_{\hat{\boldsymbol{\xi}}_M} \mathbf{W}_T^M \mathbf{G}_T^M(\hat{\boldsymbol{\xi}}_M) = \mathbf{0}, \quad (30)$$

which corresponds to the first order conditions of

$$\hat{\boldsymbol{\xi}}_M = \underset{\boldsymbol{\xi}_M \in \Theta_M}{\operatorname{argmin}} \mathbf{G}_T(\boldsymbol{\xi}_M)' \mathbf{W}_T^M \mathbf{G}_T(\boldsymbol{\xi}_M). \quad (31)$$

Furthermore, the estimates  $\hat{\boldsymbol{\xi}}_P$  obey

$$\left. \frac{\partial \mathbf{G}_T^P(\boldsymbol{\xi}_M, \boldsymbol{\xi}_P)'}{\partial \boldsymbol{\xi}_P} \right|_{\hat{\boldsymbol{\xi}}_P, \hat{\boldsymbol{\xi}}_M} \mathbf{W}_T^P \mathbf{G}_T^P(\hat{\boldsymbol{\xi}}_M, \hat{\boldsymbol{\xi}}_P) = \mathbf{0}, \quad (32)$$

which corresponds to the first order conditions of

$$\hat{\boldsymbol{\xi}}_P = \underset{\boldsymbol{\xi}_P \in \Theta_P}{\operatorname{argmin}} \mathbf{G}_T(\hat{\boldsymbol{\xi}}_M, \boldsymbol{\xi}_P)' \mathbf{W}_T^P \mathbf{G}_T(\hat{\boldsymbol{\xi}}_M, \boldsymbol{\xi}_P). \quad (33)$$

LRR parameter estimates based on disentangled macro and financial moment matches can thus be obtained by a two-step GMM/SMM estimation procedure. Since the procedure is equivalent to the generic GMM problem in Equation (29), standard

asymptotic GMM inference on  $\mathbf{G}_T(\hat{\boldsymbol{\xi}})$  and  $\hat{\boldsymbol{\xi}}$  applies (cf. Hansen, 1982, Theorem 3.1 and Lemma 4.1).

It turns out that disentangling the macro and financial moment matches is necessary for successful estimation of the LRR model. Yet, we still have to find informative and empirically useable macro and financial moment matches. Only then will the optimization problems in each step be well-defined. The next section focuses on the macro moment matches  $\mathbf{G}_T^M$ , then we motivate the financial moment matches  $\mathbf{G}_T^P$ . In both cases, the moment matches will reflect the key characteristics of the LRR model structure.

### 3.3 Analytical macro moment matches

To estimate the parameters of the dynamic system (1)–(4) by GMM using the two observable series  $g_t$  and  $g_{d,t}$ , we must construct moment matches that can capture the characteristic features of the LRR model. For that purpose, it is natural to match first and second moments, which can be analytically expressed as functions of a subset of  $\boldsymbol{\xi}_M$  that does not include the SV parameters. In particular, we can employ the following moment matches:

$$\mathbf{G}_T^{M_1}(\boldsymbol{\xi}_{M_*}) = \frac{1}{T} \sum_{t=1}^T \begin{bmatrix} g_t - \mu_c \\ g_{d,t} - \mu_d \\ g_t^2 - \mu_c^2 - \frac{\varphi_e^2 \sigma^2}{1 - \rho^2} - \sigma^2 \\ g_{d,t}^2 - \mu_d^2 - \phi^2 \frac{\varphi_e^2 \sigma^2}{1 - \rho^2} - \varphi_d^2 \sigma^2 \\ g_{d,t} g_t - \mu_c \mu_d - \phi \frac{\varphi_e^2 \sigma^2}{1 - \rho^2} \end{bmatrix}, \quad (34)$$

where  $\boldsymbol{\xi}_{M_*} = (\mu_c, \mu_d, \rho, \sigma, \varphi_e, \phi, \varphi_d)'$ .

The defining feature of the LRR model is the latent growth component  $x_t$ , a small but persistent driver of consumption and dividend growth. If such a component is

present, the observed consumption and dividend growth series exhibit small positive serial correlations, which prevail over many lags. Figure 2 provides an illustration.

[Insert Figure 2 about here]

This key LRR model characteristic can be captured only by moment matches that use auto-moments of a high lag order. We therefore consider the following moment matches that involve (cross) auto-moments of consumption and dividend growth:

$$\mathbf{G}_T^{M_2}(\boldsymbol{\xi}_{M_*}) = \begin{bmatrix} \frac{1}{T-1} \sum_{t=1}^{T-1} g_{t+1}g_t - \mu_c^2 - \rho \frac{\varphi_e^2 \sigma^2}{1-\rho^2} \\ \vdots \\ \frac{1}{T-L_1} \sum_{t=1}^{T-L_1} g_{t+L_1}g_t - \mu_c^2 - \rho^{L_1} \frac{\varphi_e^2 \sigma^2}{1-\rho^2} \\ \frac{1}{T-1} \sum_{t=1}^{T-1} g_{d,t+1}g_{d,t} - \mu_d^2 - \phi^2 \rho \frac{\varphi_e^2 \sigma^2}{1-\rho^2} \\ \vdots \\ \frac{1}{T-L_2} \sum_{t=1}^{T-L_2} g_{d,t+L_2}g_{d,t} - \mu_d^2 - \phi^2 \rho^{L_2} \frac{\varphi_e^2 \sigma^2}{1-\rho^2} \\ \frac{1}{T-1} \sum_{t=1}^{T-1} g_{d,t+1}g_t - \mu_c \mu_d - \phi \rho \frac{\varphi_e^2 \sigma^2}{1-\rho^2} \\ \vdots \\ \frac{1}{T-L_3} \sum_{t=1}^{T-L_3} g_{d,t+L_3}g_t - \mu_c \mu_d - \phi \rho^{L_3} \frac{\varphi_e^2 \sigma^2}{1-\rho^2} \end{bmatrix}, \quad (35)$$

where  $L_1$ ,  $L_2$ , and  $L_3$  denote the maximum lag orders for the respective (cross) auto-moments. Bansal and Yaron's (2004) reasoning suggests that the lag orders should be high, to capture the persistence of the series induced by  $x_t$ .

The theoretical moments that we match in Equation (35) are derived analytically and expressed as functions of the parameters. Thus, GMM estimation can be performed using  $\mathbf{G}_T^M = (\mathbf{G}_T^{M_1'}, \mathbf{G}_T^{M_2'})'$  for the first-step objective function in Equation (31). The moment matches  $\mathbf{G}_T^{M_1}$  and  $\mathbf{G}_T^{M_2}$  are valid, regardless of whether SV prevails. However, this also implies that these moment matches cannot identify the SV parameters. Constantinides and Ghosh (2011) use the higher order moments

$$\mathbf{G}_T^{M_3}(\boldsymbol{\xi}_M) = \begin{bmatrix} \frac{1}{T} \sum_{t=1}^T g_t^4 - \mathbb{E}[g_t^4; \boldsymbol{\xi}_M] \\ \frac{1}{T} \sum_{t=1}^T g_{d,t}^4 - \mathbb{E}[g_{d,t}^4; \boldsymbol{\xi}_M] \end{bmatrix}, \quad (36)$$

for the estimation of the SV parameters, where the fourth moments are analytically expressed as functions of the parameters (for details see Equations (A-1) and (A-2) in the appendix). We revisit the estimation of the SV parameters in Section 3.5.

### 3.4 Theory-based financial moment matches

We now turn to finding moment matches  $\mathbf{G}_T^P$  for the estimation of the preference parameters  $\boldsymbol{\xi}_P$  in the second step. For that purpose, we continue to pursue the philosophy to transfer key model characteristics into informative moment matches. In the present case, this amounts to exploiting asset pricing and prediction relationships implied by the LRR model. The model contains three observable financial variables, the log market return  $r_m$ , the log risk-free rate  $r_f$ , and the log price-dividend ratio  $z_m$ , which represent the candidates for moment matches. To motivate our first moment match, we use Equation (6) to price the risk-free rate, which yields

$$\mathbb{E}_t(M_{t+1}) = \frac{1}{R_{f,t+1}}, \quad (37)$$

where  $M_{t+1}$  is given in Equation (7). Applying the law of total expectation leads to the unconditional moment constraint

$$\mathbb{E}(M) = \mu_M = \mathbb{E}\left(\frac{1}{R_f}\right). \quad (38)$$

Because  $\mathbb{E}(M)$  cannot be expressed analytically as a function of the parameters, we match the mean of the simulated SDF with the sample mean of the inverse gross risk-free rate, viz:

$$\mathbf{G}_T^{P_1}(\boldsymbol{\xi}_M, \boldsymbol{\xi}_P) = \begin{bmatrix} \frac{1}{T} \sum_{t=1}^T \frac{1}{R_{f,t}} - \mu_M \\ \mu_M - \frac{1}{T} \sum_{s=1}^T M_s(\boldsymbol{\xi}_M, \boldsymbol{\xi}_P) \end{bmatrix}. \quad (39)$$

To motivate our second financial moment match, we price the market excess return  $(R_m - R_f)$  using Equation (6), apply the law of total expectation, and rearrange terms to obtain the moment condition

$$\mathbb{E}(R_m - R_f) = -\frac{\mathbb{E}[(M - \mu_M)(R_m - R_f)]}{\mu_M}. \quad (40)$$

Thus, we can use the following match of sample and simulated moments:

$$\begin{aligned} \mathbf{G}_T^{P_2}(\boldsymbol{\xi}_M, \boldsymbol{\xi}_P) &= \frac{1}{T} \sum_{t=1}^T (R_{m,t} - R_{f,t}) \\ &+ \frac{\frac{1}{\mathcal{T}(T)} \sum_{s=1}^{\mathcal{T}(T)} [R_{m,s}(\boldsymbol{\xi}_M, \boldsymbol{\xi}_P) - R_{f,s}(\boldsymbol{\xi}_M, \boldsymbol{\xi}_P)] [M_s(\boldsymbol{\xi}_M, \boldsymbol{\xi}_P) - \mu_M]}{\mu_M}. \end{aligned} \quad (41)$$

The set of test assets can be extended by including managed portfolios, as suggested by [Cochrane \(1996\)](#). Given a vector of instruments available at  $t$ ,  $\mathbf{Z}_t$ , pricing the managed portfolio payoffs  $(R_{m,t+1} - R_{f,t+1})\mathbf{Z}_t$  using Equation (6) implies:

$$\mathbb{E}[(R_{m,t+1} - R_{f,t+1})\mathbf{Z}_t] = -\frac{\mathbb{E}[(M_{t+1} - \mu_M)(R_{m,t+1} - R_{f,t+1})\mathbf{Z}_t]}{\mu_M}.$$

To use the resulting moment matches for SMM,  $\mathbf{Z}_t$  needs to be determined within the LRR model, because the instruments have to be simulated, too. One could, for instance, follow [Constantinides and Ghosh \(2011\)](#) and construct a managed portfolio that uses  $\mathbf{Z}_t = r_{f,t}$ .<sup>7</sup>

For a third financial moment match, we consider the unconditional Sharpe-Ratio of the market portfolio, as it is a key statistic for the risk-return trade-off implied by the LRR model. The means of the market excess return and the risk-free rate

---

<sup>7</sup>Note that a predictive relationship between the price-dividend ratio and future excess returns is not a feature of the LRR model, so  $z_{m,t}$  cannot be used as an instrument for the construction of a managed portfolio or in a predictive regression.

are accounted for in Equations (39) and (41), so the only remaining moment to be matched is the expected value of the squared market excess return:

$$\begin{aligned} \mathbf{G}_T^{P_3}(\boldsymbol{\xi}_M, \boldsymbol{\xi}_P) &= \frac{1}{T} \sum_{t=1}^T (R_{m,t} - R_{f,t})^2 \\ &\quad - \frac{1}{\mathcal{T}(T)} \sum_{s=1}^{\mathcal{T}(T)} (R_{m,s}(\boldsymbol{\xi}_M, \boldsymbol{\xi}_P) - R_{f,s}(\boldsymbol{\xi}_M, \boldsymbol{\xi}_P))^2. \end{aligned} \quad (42)$$

Our final financial moment matches are motivated by a prediction relation pointed out by [Campbell and Shiller \(1988\)](#). They argue that the linear approximations in Equations (8) and (9) imply that the log price-dividend ratio predicts future discount rates.<sup>8</sup> We make use of this predictive relationship by matching the slope parameter of a regression of the risk-free rate on past values of the log price-dividend ratio, which entails matching the first and the second moments of  $z_{m,t}$  too:

$$\mathbf{G}_T^{P_4}(\boldsymbol{\xi}_M, \boldsymbol{\xi}_P) = \begin{bmatrix} \frac{\frac{1}{T-1} \sum_{t=1}^{T-1} [R_{f,t+1} - \frac{1}{T-1} \sum_{t=1}^{T-1} R_{f,t+1}] z_{m,t}}{\frac{1}{T} \sum_{t=1}^T (z_{m,t} - \frac{1}{T} \sum_{t=1}^T z_{m,t})^2} \\ - \frac{\frac{1}{\mathcal{T}(T)-1} \sum_{s=1}^{\mathcal{T}(T)-1} [z_{m,s}(\boldsymbol{\xi}_M, \boldsymbol{\xi}_P) - \mu_{1,z_m}] R_{f,s+1}(\boldsymbol{\xi}_M, \boldsymbol{\xi}_P)}{\mu_{2,z_m} - \mu_{1,z_m}^2} \\ \frac{1}{T} \sum_{t=1}^T z_{m,t} - \mu_{1,z_m} \\ \frac{1}{T} \sum_{t=1}^T z_{m,t}^2 - \mu_{2,z_m} \\ \mu_{1,z_m} - \frac{1}{\mathcal{T}(T)} \sum_{s=1}^{\mathcal{T}(T)} z_{m,s}(\boldsymbol{\xi}_M, \boldsymbol{\xi}_P) \\ \mu_{2,z_m} - \frac{1}{\mathcal{T}(T)} \sum_{s=1}^{\mathcal{T}(T)} z_{m,s}^2(\boldsymbol{\xi}_M, \boldsymbol{\xi}_P) \end{bmatrix}. \quad (43)$$

The stacked financial moment matches  $\mathbf{G}_T^P = \left( \mathbf{G}_T^{P_1'}, \mathbf{G}_T^{P_2'}, \mathbf{G}_T^{P_3'}, \mathbf{G}_T^{P_4}' \right)'$  will be used for the SMM objective function in Equation (33).<sup>9</sup>

[Insert Table 5 about here]

<sup>8</sup>A simulation exercise shows that the predictive power of  $z_{m,t}$  for  $R_{f,t+1}$  is strong: The  $R^2$  of a one-step predictive regression is 95%. The simulation is based on the parameter values given in Table 2 and a simulated sample size of  $10^6$  observations.

<sup>9</sup>As pointed out by [Parker and Julliard \(2005\)](#), we must ensure that the auxiliary parameters  $\mu_M$ ,  $\mu_{1,z_m}$ , and  $\mu_{2,z_m}$  in Equations (39) and (43) are exactly matched, which can be achieved by inserting the simulated means into the respective moment conditions.

The moment sensitivity analysis in Table 5 shows which of the financial moment matches provides information about which parameter values. All simulated moments respond strongly to a 10% change in the subjective discount factor  $\delta$ . For both  $\gamma$  and  $\psi$ , one of the moments responds sizably to a specific parameter change, whereas all other moments do not. Most information about  $\gamma$  is contained in the LRR model's pricing implication for the market excess return, which is reflected in the 10% decrease in the simulated moment in Equation (41) in response to a 10% decrease in  $\gamma$ . The other simulated moments are not particularly sensitive to  $\gamma$ . The identification of the IES  $\psi$  is mainly provided by the slope parameter of the predictive regression of  $R_{f,t+1}$  on  $z_{m,t}$ . The corresponding simulated moment responds to a 10% decrease in  $\psi$  by a 14% increase; the other moments change by 4% or less. The prediction moment is not sensitive to a change in  $\gamma$ , which thus helps disentangle risk aversion and the intertemporal elasticity of substitution.

### 3.5 Concentrating out stochastic volatility

The estimation of the parameters of stochastic volatility processes is a topic of substantial discussion in econometrics. The methodological challenges are aggravated in the LRR model, because stochastic consumption volatility is just one ingredient of this non-linear multiple-equation system. We have seen in Section 3.1 that the ad hoc moment matches based on the moments in Panel A-2 of Table 1 are not useful to identify the SV parameters. The theory-based moment matches presented in the previous section cannot do a better job because these matches are based on unconditional moment constraints, and stochastic volatility is about changing conditional variances. We have also seen that the analytical moment matches proposed in Section 3.3 can be used to identify the unconditional variance  $\sigma^2$ , but not the SV parameters  $\nu_1$  and  $\sigma_w$ . As previously mentioned, we could exploit the higher order



moments of dividend and consumption growth in (A-1) and (A-2) (as suggested by Constantinides and Ghosh, 2011) to identify the SV parameters, which are functions of the SV parameters. However, a simulation study for the estimation of the SV parameters  $\nu_1$  and  $\sigma_w$  only, assuming the true values of all other macro parameters to be known, yields starting value dependent results, which indicates that these moment conditions are not sufficiently informative to identify the SV parameters.<sup>10</sup>

Instead of looking for more sophisticated ways to estimate the SV parameters, we propose to simplify the problem. Table 4 shows that even large changes in  $\nu_1$  and  $\sigma_w$  have only a small impact on the unconditional equity premium. If the primary interest is not the estimation of the SV parameters and the evolution of the conditional risk premium but rather the estimation of the preference parameters and the model-implied risk premium, an alternative estimation strategy could “concentrate out” the SV parameters. In a simulation of the model in the course of SMM estimation, the stochastic volatility  $\sigma_t^2$  is replaced by its unconditional expectation  $\mathbb{E}(\sigma_t^2) = \sigma^2$ , which is estimated in the first step. We posit that the unconditional moments of the simulated financial variables (and the measurable functions of them used for moment matching) would not be greatly affected when  $\sigma_t^2$  is replaced by  $\sigma^2$ . Concentrating out SV might reduce efficiency, yet it can also enhance robustness, because the SV parameters may be poorly identified by weak moment conditions and/or a small sample size. In Section 4.3, we assess our estimation strategy in a simulation study and quantify the loss in efficiency.

---

<sup>10</sup>When testing other candidates, such as the auto-moments of the squared market return or the fourth moments of returns, the result remains the same.

## 4 Simulation study

### 4.1 General setup

We evaluate our methodological approach in an extensive simulation study. For that purpose, we generate data by simulating series of varying length  $T$  for  $g$ ,  $g_d$ ,  $r_m$ ,  $r_f$ , and  $z_m$ , as implied by the LRR model. The values assumed for the true macro parameters  $\xi_M$  and the preference parameters  $\xi_P$  are those calibrated by [Bansal and Yaron \(2004\)](#). They are listed in [Table 2](#).

The length of the simulated series varies from  $T = 1000$  to  $T = 100,000$ . Assuming a monthly sampling frequency,  $T = 1000$  is equivalent to about 83 years, which is a large, yet reasonable size for a real-world application. The longer series serve to illustrate the behavior of the estimates for a growing sample size. We restrict  $\hat{\varphi}_e$ ,  $\hat{\phi}$ , and  $\hat{\varphi}_d$  to positive values, while  $\hat{\rho}$ ,  $\hat{\mu}_c$ , and  $\hat{\mu}_d$  must take values between 0 and 1. For a good approximation of the simulated moments, we use  $\mathcal{T}(T) = 10^6$ . To minimize the GMM and SMM objective functions, we use the Nelder-Mead simplex algorithm.

To assess the estimation precision, we generate 400 replications for each  $T$ . In [Section 2.2](#) we discussed the inherent fragility of the LRR model, which may be insoluble for certain parameter combinations that may be used in the course of SMM estimation. A practical solution would be a penalty term that moves the optimizer away from those unfavorable parameter combinations. To economize computation time in the simulation study, we choose not to use a penalty term but instead drop any replications for which the optimizer stops at an unsolvable model. When applying the method to real data, a penalty term should be used.

In [Section 3.1](#) we saw that the estimation approaches based on the moments in [Table 1](#) yielded unreliable results, and we have emphasized the danger of reporting

overly optimistic estimates that result from a convergence to a point near plausibly chosen starting values. It is crucial to avoid that fallacy. Prior to engaging in our large-scale simulation study, we therefore carefully tested our proposed two-step estimation procedure. We started the optimization in each step from different starting values using a variety of test data to ensure that the optimization algorithm converges to identical values. Panel C in Table 3 provides an illustration. Using the same data we relied on for the failed estimation attempts reported in Panel A and B, the two-step GMM/SMM procedure yields the same estimates, regardless of the initial values chosen. The objective functions within the two-step estimation procedure become well defined, such that the application of sophisticated optimizers becomes unnecessary.

## 4.2 GMM estimation of the macro parameters

For each simulated time series, we perform eight GMM estimations of  $\xi_{M^*}$ , using  $\mathbf{W}_T = \mathbf{I}$  and the macro moment matches in Table 6. The number of moments used ranges from exact identification (7 mc) to ample overidentification (185 mc). Each set of them includes the first and second moment matches of Equation (34) and a varying number of (cross) auto-moments from Equation (35). The maximum lag order is  $L_1 = L_2 = L_3 = 60$ , meaning that we account for autocovariances up to five years, assuming a monthly frequency. The estimation of the macro parameters should benefit from allowing for high lag orders for the autocovariances, because the drivers of the LRR macro dynamics are slow-moving processes.

To ensure the feasibility of our simulation study, in which we conduct  $400 \times 8 \times 4$  estimations, we use one vector of starting values only. The initial robustness checks provide confidence that starting value dependence is not an issue for the moment matches we advocate. Nevertheless, we purposefully choose starting values that

are at some distance from the true parameters.<sup>11</sup> A poor starting point makes the problem harder for the optimization algorithm, and more time-consuming, but it also prevents the danger of reporting overly optimistic results.

Tables 7–10 report the means and standard deviations of the macro parameter estimates computed across the 400 replications. Figures 3 and 4 illustrate the estimation quality using kernel densities.

[Insert Table 6 about here]

[Insert Tables 7 through 10 about here]

[Insert Figures 3 and 4 about here]

As we can see, estimation precision varies across parameters. For  $\rho$ ,  $\varphi_e$ , and  $\phi$ , both a relatively large sample size ( $T > 2000$ ) and informative moment conditions are needed for precise results (cf. Tables 8 and 9), whereas  $\mu_c$ ,  $\sigma$ , and  $\varphi_d$  are less difficult to estimate (cf. Tables 7, 9, and 10). The finite sample simulation evidence indicates that the favorably small asymptotic standard errors reported in empirical estimations of LRR models should be taken with a grain of salt. These applications use a much smaller sample size.

Although the precision of the parameter estimates naturally improves with the sample size, for the critical parameters  $\rho$ ,  $\varphi_e$ , and  $\phi$  it can also be enhanced by increasing the maximum lag orders  $L_1$ ,  $L_2$ , and  $L_3$ . The ability to estimate  $\rho$  precisely is crucial, because the persistent growth component  $x_t$  determines the dynamics of all macroeconomic and financial variables in the LRR model. Large sample sizes in the range of  $T = 5000$  are yet unattainable in real-world applications, such that the availability of informative moment conditions that prove to be useful in small samples too is of utmost importance.

---

<sup>11</sup>We use  $\xi_{M_*} = (0.018, 0.018, 0.881, 0.082, 0.003, 7.389, 7.389)'$  as starting values.

For small samples, a moderate increase in the number of moment conditions (e.g. up to 35 mc) does not improve the parameter estimates. In contrast, an increase of the maximum lag order from three (113 mc) to five years (185 mc) still has some beneficial effect. The same conclusion arises when we consult the kernel density plots in Figures 3 and 4, which compare four different moment sets: 7 mc, 35 mc, 87 mc, and 185 mc. We observe that the larger moment sets are particularly useful to improve the estimation quality for the critical parameters  $\rho$ ,  $\phi$ , and  $\varphi_e$ .

To determine formally the optimal lag order, we propose selecting the moment set that minimizes the Bayes-Schwarz information criterion (BIC) for GMM suggested by Andrews (1999):

$$\text{GMM-BIC} = J_T - (|c| - p_b) \ln T, \quad (44)$$

where  $J_T$  is Hansen's (1982) J-statistic,  $|c|$  stands for the number of moment conditions, and  $p_b$  indicates the number of parameters.

[Insert Table 11 about here]

Table 11 shows that in the vast majority of replications, the GMM-BIC selects the largest moment set (185 mc), confirming our previous findings. Because we simulate error-free LRR model data, GMM-BIC correctly points to the highest lag order. Real data, consumption in particular, will be error-prone, and the applied researcher will face the familiar trade-off between efficiency (allowing for a high lag order) and robustness (avoid picking up noise). Tables 7–10 show that the improvement of estimation quality from 35 mc (max. lags < 1 year) to 87 mc (max. lags: 3 years) is considerable, while the smaller incremental benefits of using 185 mc (max. lags: 5 years) may be offset by error-prone data. For practical applications, we therefore recommend using a moderately high lag order.

Replications for which the optimization algorithm failed to converge or produced economically implausible results are not included in Tables 7–10 and the kernel plots in Figures 3 and 4. We consider a result implausible if one of the values to which the optimizer converges differs from the true parameter by a factor of 10 or more.<sup>12</sup>

[Insert Table 12 about here]

Table 12 shows that the number of successful estimations tends to be smaller for shorter time series and the parsimonious moment sets. It is not surprising that estimation problems are exacerbated in small samples. We seek to estimate the parameters of highly persistent latent processes, which is hard to detect for small  $T$ . However, Table 12 also shows that this problem can be mitigated by including more informative moment conditions. For any sample size  $T$ , the use of a higher lag order for the auto-moments increases the number of successful estimations.

The exclusion of the problematic replications entails a sample selection effect that actually strengthens the previous conclusions. The extended moment sets facilitate the computation of estimates on problematic data, for which the more parsimonious moment matches fail. Because data of the more problematic, less informative replications yield worse estimates, the benefit offered by using the extended moment sets is even understated.

### 4.3 SMM estimation of the preference parameters

To estimate the preference parameters  $\boldsymbol{\xi}_P = (\delta, \gamma, \psi)'$ , we use the six theory-based financial moment matches  $\mathbf{G}_T^{P_1}$ ,  $\mathbf{G}_T^{P_2}$ ,  $\mathbf{G}_T^{P_3}$ , and  $\mathbf{G}_T^{P_4}$  in the SMM objective function (33). Stochastic volatility is present in the simulated data, but for the estima-

---

<sup>12</sup>In an application using an empirical data, we might try to tackle the problematic data using the remedies of applied econometrics, such as using different (and more favorable) starting values, probing alternative optimization algorithms and tuning the algorithm’s parameters. However, such a clinical handling of the problematic simulated data sets is impossible in a large-scale simulation study.

tion we concentrate out the SV parameters, as described in Section 3.5. We perform the SMM estimation using the first-step macro parameter estimates that are based on the 185 mc moment set.

We also consider the hypothetical case that the true macro parameters are known, either the complete parameter vector  $\boldsymbol{\xi}_M$ , which includes all SV parameters, or the subset  $\boldsymbol{\xi}_{M^*}$ , which excludes  $\nu_1$  and  $\sigma_w$ . Contrasting the SMM estimates obtained when concentrating out SV with the estimates that result from assuming the complete vector of macro parameters as known (such that we can compute  $\sigma_t^2$  when simulating the theory-based moments) allows us to quantify the efficiency losses of our proposed estimation strategy. By comparing the SMM results based on estimated versus true  $\boldsymbol{\xi}_{M^*}$ , we can assess the quality of the financial moment matches independent of the effect of potentially imprecise first-step estimates. We also contrast the results using the theory-based moment matches with those based on the six ad hoc moment matches in Panel A-2 of Table 1. For each estimation attempt, we perform an initial grid search over reasonable ranges of the three preference parameters, and use the parameter combination that yields the smallest SMM objective as starting values for the Nelder-Mead simplex algorithm.

[Insert Table 13 about here]

[Insert Figure 5 about here]

Panel A of Table 13 displays means and standard deviations of the SMM estimates of the preference parameters that use the true macro parameters for the simulation of moments. The first column reports the results based on the ad hoc moment matches, the second contains the results for the theory-based moment matches. In both cases, the estimates are obtained by concentrating out stochastic volatility, i.e. using  $\sigma = \mathbb{E}(\sigma_t^2)$  instead of  $\sigma_t^2$  for SMM. The third column of Panel A contains

the SMM estimation results assuming the complete vector of macro parameters as known, and thus using  $\sigma_t^2$  when simulating the theory-based financial moments. Figure 5 compares the estimation quality of the ad hoc moment matches with the theory-based moment matches by means of kernel density estimates.

We observe that the estimation quality delivered by SMM is surprisingly good. Bias and standard deviation of the preference parameter estimates are quite small; the kernel density estimates allocate probability masses around the true parameters also for small  $T$ . The subjective discount factor  $\delta$  can be estimated most precisely, but the estimates of the relative risk aversion parameter  $\gamma$  are also quite accurate. The estimation quality delivered by theory-based moment matches outperforms the ad hoc moment matches, most prominently for the estimate of  $\psi$ . The theory-based moment matches thus prove to be particularly useful for disentangling risk aversion and intertemporal elasticity of substitution. Comparing the second and third column of Panel A in Table 13, it is striking that the estimation quality of the preference parameters is barely affected by concentrating out stochastic volatility, which corroborates our proposed estimation strategy.

[Insert Figure 6 about here]

Panel B of Table 13 displays the means and standard deviations of the SMM preference parameter estimates that use the estimated macro parameters for the simulation of moments. We observe that the theory-based moment matches remain superior to the ad hoc moment matches. We also note that the estimation precision for the subjective discount factor is not much hampered by replacing the true macro parameters by the first-step estimates. Parameter standard deviations and bias remain small even for  $T = 1000$ . Estimating relative risk aversion and IES based on estimated macro parameter poses a greater challenge. Compared with the estimates



that rely on the true macro parameters, bias and standard deviation increase considerably. But we also observe that the kernel densities for the preference parameter estimates in Figure 6 retain their mode at the true values, and that the probability mass is still centered around the true parameter value. This observation leads to the conclusion that outlier estimates of  $\gamma$  and  $\psi$  are responsible for the increase of standard deviation and bias of the preference parameter estimates

These results demonstrate the importance of using precise macro parameter estimates as input for the SMM estimation of the preference parameters. To improve the quality of the first-step input, we consider two strategies. First, the accuracy of the first-step GMM estimates could be increased by using a more efficient weighting. In particular, we could use an estimate of the efficient GMM weighting matrix  $\mathbf{W}_e^M = \left(\text{Var}(\mathbf{G}_T^M(\hat{\boldsymbol{\xi}}_{M_*}))\right)^{-1}$  and hope that the asymptotic efficiency gains also kick in for smaller sample sizes. Second, we could raise the bar for the quality of the first-step macro estimates and discard those that do not fulfill the requirements. The effect of both strategies can be studied in Table 14 and again in the kernel plots of Figure 6.

[Insert Table 14 about here]

Panel A of Table 14 shows the SMM estimation results for the preference parameters that are based on “efficient” macro parameter estimates. These estimates are obtained by a two-stage GMM procedure. The first stage uses  $\mathbf{W}_T^M = \mathbf{I}$  in Equation (31) to get an initial estimate of  $\boldsymbol{\xi}_{M_*}$ , which is then used to compute an estimate of the efficient GMM weighting matrix  $\mathbf{W}_e^M$ . Second-stage GMM estimates of  $\boldsymbol{\xi}_{M_*}$  result from using  $\mathbf{W}_T^M = \widehat{\mathbf{W}}_e^M$  in Equation (31). Comparing Panel A of Table 14 with Panel B of Table 13 shows the improvement when using “efficient” macro estimates for the SMM estimation of the preference parameters. Estimation precision improves particularly for the empirically relevant small sample size and for the pref-

erence parameters that are difficult to estimate, namely  $\gamma$  and  $\psi$ . The kernel plots in Figure 6 show how the preference parameter estimates based on the “efficient” macro estimates concentrate more closely around the true values. The kernel plots also show that the likelihood of severe overestimations of  $\gamma$  and  $\psi$  is reduced, which explains the beneficial effect on bias and standard deviation of the preference parameter estimates.<sup>13</sup>

Panel B of Table 14 and again Figure 6 reveal the incremental effect of raising the bar for the quality of first-step GMM estimates before allowing to enter the SMM estimation. For that purpose, we discard a replication if one of the macro parameter estimates is more than twice its true value. We observe that the quality of the preference parameter estimates further improves. The kernel plots in Figure 6 show that the number of outlier estimates is further reduced and the mass of the distributions shifts more closely around the true parameters. Of course, such a procedure is only useable in a simulation study. A practical application would require a judgment call based on size and standard errors of the first-step macro estimates. If these estimates are considered implausible, or too imprecise, one would then refrain from entering the second estimation step.

## 5 Discussion and conclusion

Estimating an asset pricing model that features two latent processes as fundamental economic drivers, as well as a pricing kernel that depends on unobservable variables, is a demanding job for financial econometrics. The bar is raised if such a model must be solved every time it is computed for new values of the model parameters, and if it is possible that the solution does not exist. Add as a final obstacle that

---

<sup>13</sup>N.b. that the major improvements of the macro parameter estimates result from well-chosen moment matches rather than from applying an efficient weighting scheme. Weighting is no panacea; it cannot compensate for ill-conceived moment matches.

the number of observations available for empirical analysis is small, and you have collected the hurdles to empirical tests of long-run risk asset pricing models. As an estimation technique, SMM is designed to cope with such methodological challenges. It combines a compelling estimation philosophy—matching sample moments and their model-implied counterparts—with computational feasibility. The model-implied moments need not be analytically expressed as functions of the parameters but instead can be approximated by sample means of the simulated model series.

Although SMM is thus appealing for our purpose, some empirically important questions have not been addressed in prior literature, and our study aims to close that gap. Are the moments selected for matching informative enough to identify the deep model parameters that describe the dynamics of latent processes and investor preferences? Non-identification may hide well in such a complex model structure. Even powerful optimizers fail on an objective function surface with myriads of local minima, implied by weakly identifying moment conditions. This caveat calls for due diligence when transferring the key model characteristics into informative moment matches. Even if meaningful, theory-rooted, and practically useable moment conditions can be found, what sample size is required to deliver precise estimates?

We tackle these issues by proposing a combined GMM/SMM two-step estimation strategy, in which we elicit moment matches that reflect the key features of the LRR model. We first estimate the parameters that drive the macroeconomic dynamics, and then deal with investor preference parameters in a second step, using the first-step estimates as input and exploiting the asset pricing equations and predictive relations implied by the LRR framework. The question of how large the number of observations must be for a successful estimation is addressed in an extensive simulation study.

The theoretical moments that we use in the first estimation step can be analytically expressed as functions of the macro parameters, such that GMM estimation becomes feasible. These moment matches are valid in the presence of stochastic consumption volatility, but they cannot identify the SV parameters. They can, however, identify the unconditional consumption volatility, which is required in the second estimation step. The properties of the latent persistent growth component, the defining feature of the LRR model, are captured by including remote lags of (cross-) autocovariances of consumption and dividend growth, which considerably improves the parameter estimates.

Considering the notorious difficulty associated with estimating stochastic volatility processes, we propose to concentrate out the SV parameters in the second (SMM) estimation step. We do not preclude the potential prevalence of SV in the data, but we replace time-varying stochastic volatility with the first-step unconditional volatility estimate when computing the simulated moments in the second step. Unless the focus is on conditional pricing implications, estimating the preference parameters is feasible without loss of precision.

Using the proposed theory-based moment matches, SMM delivers precise estimates for the subjective discount factor, relative risk aversion, and the intertemporal elasticity of substitution even for smaller samples. Considering the complexity of the LRR asset pricing equations, this result is encouraging. SMM lives up to the promise of being able to deliver good estimates in a difficult setup, provided that a well thought-out moment matching strategy is used.

The first caveat is that the recursive LRR model structure must be reflected in the estimation strategy, meaning that the interlacement of the moment matches has to be disentangled. We achieve this by the proposed GMM/SMM two-step estimation strategy. For an accurate estimation of the preference parameters, the

estimates of the macro parameters used for the second estimation step must be of good quality. For that purpose, both informative first-step moment matches and a relatively large sample size are required. This conclusion challenges empirical applications, which inevitably involve small samples. It may sound like a truism, but to estimate a complex DAPM like the LRR model informative data (long time series) and strong moment matches are indispensable. If the data and/or estimation quality of the macroeconomic parameters is poor, researchers cannot expect much from the second-step estimation of the preference parameters. Refraining from estimating them in the first place is the scientifically honest decision. Our two-step approach thus constitutes a reality check for applied work.

Fruitful extension in subsequent research could seek to increase the quality of the macro parameter estimates. Time has to pass until confidence bounds will narrow, but strong and well thought-out moment matches will help applied research in the meantime.

## References

- Andersen, T. G., Chung, H.-J., Sørensen, B. E., 1999. Efficient method of moments estimation of a stochastic volatility model: A Monte Carlo study. *Journal of Econometrics* 91 (1), 61–87.
- Andrews, D. W. K., 1999. Consistent moment selection procedures for generalized method of moments estimation. *Econometrica* 67 (3), 543–563.
- Bansal, R., Gallant, A. R., Tauchen, G., 2007a. Rational pessimism, rational exuberance, and asset pricing models. *The Review of Economic Studies* 74 (4), 1005–1033.
- Bansal, R., Kiku, D., Yaron, A., 2007b. Risks for the long run: Estimation and inference, Working Paper.
- Bansal, R., Shaliastovich, I., 2013. A long-run risks explanation of predictability puzzles in bond and currency markets. *The Review of Financial Studies* 26 (1), 1–33.
- Bansal, R., Yaron, A., 2004. Risks for the long run: A potential resolution of asset pricing puzzles. *The Journal of Finance* 59 (4), 1481–1509.
- Campbell, J. Y., Shiller, R. J., 1988. The dividend-price ratio and expectations of future dividends and discount factors. *The Review of Financial Studies* 1 (3), 195–228.
- Chen, S. X., 1999. Beta kernel estimators for density functions. *Computational Statistics & Data Analysis* 31 (2), 131–145.
- Cochrane, J. H., 1996. A cross-sectional test of an investment-based asset pricing model. *Journal of Political Economy* 104 (3), 572–621.

- Constantinides, G. M., Ghosh, A., 2011. Asset pricing tests with long-run risks in consumption growth. *The Review of Asset Pricing Studies* 1 (1), 96–136.
- Drechsler, I., Yaron, A., 2011. What’s vol got to do with it. *The Review of Financial Studies* 24 (1), 1–45.
- Epstein, L. G., Zin, S. E., 1989. Substitution, risk aversion, and the temporal behavior of consumption and asset returns: A theoretical framework. *Econometrica* 57 (4), 937–969.
- Ferson, W., Nallareddy, S., Xie, B., 2013. The “out-of-sample” performance of long run risk models. *Journal of Financial Economics* 107 (3), 537–556.
- Gallant, A., Hsieh, D., Tauchen, G., 1997. Estimation of stochastic volatility models with diagnostics. *Journal of Econometrics* 81 (1), 159–192.
- Hansen, L. P., 1982. Large sample properties of generalized method of moments estimators. *Econometrica* 50 (4), 1029–1054.
- Hansen, N., Ostermeier, A., 2001. Completely derandomized self-adaptation in evolution strategies. *Evolutionary Computation* 9 (2), 159–195.
- Hasseltoft, H., 2012. Stocks, bonds, and long-run consumption risks. *Journal of Financial and Quantitative Analysis* 47, 309–332.
- Jacquier, E., Polson, N. G., Rossi, P. E., 2002. Bayesian analysis of stochastic volatility models. *Journal of Business & Economic Statistics* 20 (1), 69–87.
- Kim, S., Shephard, N., Chib, S., 1998. Stochastic volatility: Likelihood inference and comparison with ARCH models. *The Review of Economic Studies* 65 (3), 361–393.

- Pakoš, M., 2013. Long-run risk and hidden growth persistence. *Journal of Economic Dynamics and Control* 37 (9), 1911–1928.
- Parker, J. A., Julliard, C., 2005. Consumption risk and the cross section of expected returns. *Journal of Political Economy* 113 (1), 185–222.
- Ruiz, E., 1994. Quasi-maximum likelihood estimation of stochastic volatility models. *Journal of Econometrics* 63 (1), 289–306.
- Sandmann, G., Koopman, S. J., 1998. Estimation of stochastic volatility models via Monte Carlo maximum likelihood. *Journal of Econometrics* 87 (2), 271–301.
- Silverman, B. W., 1986. *Density estimation for statistics and data analysis*. Vol. 26. CRC press.
- Singleton, K. J., 2006. *Empirical Dynamic Asset Pricing*. Princeton University Press.



## A Appendix

### A.1 Higher order moments for SV parameter estimation

$$\begin{aligned} \text{Var} [g_{t+1}^2] &= \frac{3\varphi_e^4 \sigma_w^2 (1 + \nu_1 \rho^2)}{(1 - \rho^4)(1 - \nu_1^2)(1 - \nu_1 \rho^2)} + \frac{1}{1 - \rho^4} \left[ 2\varphi_e^4 \sigma^4 + \frac{4\rho^2 \varphi_e^4 \sigma^4}{1 - \rho^2} \right] + \frac{3\sigma_w^2}{1 - \nu_1^2} \\ &\quad + 4\mu_c^2 \frac{\varphi_e^2 \sigma^2}{1 - \rho^2} + \frac{6\varphi_e^2 \sigma_w^2 \nu_1}{(1 - \nu_1^2)(1 - \nu_1 \rho^2)} + \frac{4\varphi_e^2 \sigma^4}{1 - \rho^2} + 2\sigma^4 + 4\mu_c^2 \sigma^2 \end{aligned} \quad (\text{A-1})$$

$$\begin{aligned} \text{Var} [g_{d,t+1}^2] &= \phi^4 \left[ \frac{3\varphi_e^4 \sigma_w^2 (1 + \nu_1 \rho^2)}{(1 - \rho^4)(1 - \nu_1^2)(1 - \nu_1 \rho^2)} + \frac{1}{1 - \rho^4} \left( 2\varphi_e^4 \sigma^4 + \frac{4\rho^2 \varphi_e^4 \sigma^4}{1 - \rho^2} \right) \right] \\ &\quad + \frac{3\sigma_w^2}{1 - \nu_1^2} \varphi_d^4 + 4\mu_d^2 \frac{\varphi_e^2 \sigma^2}{1 - \rho^2} \phi^2 + \frac{6\varphi_e^2 \sigma_w^2 \nu_1}{(1 - \nu_1^2)(1 - \nu_1 \rho^2)} \phi^2 \varphi_d^2 \\ &\quad + \frac{4\varphi_e^2 \sigma^4}{1 - \rho^2} \phi^2 \varphi_d^2 + 2\sigma^4 \varphi_d^4 + 4\mu_d^2 \varphi_d^2 \sigma^2 \end{aligned} \quad (\text{A-2})$$

These expressions are a corrected version of the formulas reported by [Constantinides and Ghosh \(2011\)](#).

# Tables and Figures

**Table 1: Macro, financial and prediction moments used for assessment of previously suggested estimation strategies**

The table lists the moments for two estimation strategies that aim to estimate the deep parameters of the LRR model. The first estimation strategy in Panel A is the SMM approach adapted from [Hasseltoft \(2012\)](#), the second estimation strategy in Panel B is the GMM approach by [Constantinides and Ghosh \(2011\)](#). Panel 1 lists the moments of macroeconomic LRR variables, Panel 2 contains the moments of financial LRR variables, and Panel 3 lists the moments from a prediction relationship. Finally,  $\zeta_{t+1}$  is the residual of an AR(1) process for log consumption growth that is obtained by regressing  $g_{t+1}$  on  $g_t$ .

| Panel A – SMM approach                | Panel B – GMM approach                                 |
|---------------------------------------|--|
| <u>Panel 1: Macro moments</u>         |  |
| $\mathbb{E}(g_t)$                     | $\mathbb{E}(g_t)$                                      |
| $\mathbb{E}(g_{d,t})$                 | $\mathbb{E}(g_{d,t})$                                  |
| $\mathbb{E}(g_t^2)$                   | $\mathbb{E}(g_t^2)$                                    |
| $\mathbb{E}(g_{d,t}^2)$               | $\mathbb{E}(g_{d,t}^2)$                                |
| $\mathbb{E}(g_t g_{t+1})$             | $\mathbb{E}(g_t, g_{t+1})$                             |
| $\mathbb{E}(g_t g_{t+2})$             | $\mathbb{E}(g_{d,t}, g_{d,t+1})$                       |
|                                       | $\mathbb{E}(g_t, g_{d,t})$                             |
|                                       | $\mathbb{E}(g_t^4)$                                    |
|                                       | $\mathbb{E}(g_{d,t}^4)$                                |
| <u>Panel 2: Asset pricing moments</u> |  |
| $\mathbb{E}(r_{m,t} - r_{f,t})$       | $\mathbb{E}(M_{t+1} \cdot R_{m,t+1} - 1) = 0$          |
| $\mathbb{E}(r_{f,t})$                 | $\mathbb{E}(M_{t+1} \cdot R_{f,t+1} - 1) = 0$          |
| $\mathbb{E}(z_{m,t})$                 | $\mathbb{E}[(M_{t+1} \cdot R_{m,t+1} - 1)r_{f,t}] = 0$ |
| $\mathbb{E}[(r_{m,t} - r_{f,t})^2]$   | $\mathbb{E}[(M_{t+1} \cdot R_{m,t+1} - 1)z_{m,t}] = 0$ |
| $\mathbb{E}[r_{f,t}^2]$               | $\mathbb{E}[(M_{t+1} \cdot R_{f,t+1} - 1)r_{f,t}] = 0$ |
| $\mathbb{E}[z_{m,t}^2]$               | $\mathbb{E}[(M_{t+1} \cdot R_{f,t+1} - 1)z_{m,t}] = 0$ |
| <u>Panel 3: Prediction moments</u>    |  |
| $\mathbb{E}(\zeta_{t+1}^2)$           |  |
| $\mathbb{E}(\zeta_{t+1}^2 z_{m,t})$   |  |

**Table 2: True parameter values**

This table holds the parameter values calibrated by [Bansal and Yaron \(2004\)](#). These values are used as true parameter values for the simulation of the LRR model.

---

|             |                     |             |        |
|-------------|---------------------|-------------|--------|
| $\mu_c$     | 0.0015              | $\sigma$    | 0.0078 |
| $\mu_d$     | 0.0015              | $\phi$      | 3.0    |
| $\rho$      | 0.9790              | $\varphi_d$ | 4.5    |
| $\varphi_e$ | 0.0440              | $\delta$    | 0.998  |
| $\nu_1$     | 0.9870              | $\gamma$    | 10.0   |
| $\sigma_w$  | $2.3 \cdot 10^{-6}$ | $\psi$      | 1.5    |

---

**Table 3: Comparison of alternative strategies to estimate the LRR model**

We simulate data of length  $T = 100,000$  generated by an LRR model based on Bansal and Yaron's (2004) parameter values (cf. Table 2). We estimate the model parameters using alternative estimation approaches and three different vectors of starting values. Panel A reports the results from an SMM estimation for which we match the moments in Panel A of Table 1, Panel B provides the results obtained from adopting the GMM estimation strategy proposed by Constantinides and Ghosh (2011), matching the moments listed in Panel B of Table 1. Panel C shows the estimates from our two-step approach. We always use  $\mathbf{W}_T = \mathbf{I}$ . The starting values in  $\xi_{s_1}$  correspond to the true parameter vector,  $\xi_{s_2} = (0.0015, 0.0015, 0.95, 0.00001, 0.008, 3, 5, 0.99, 12, 1.2)'$ , and  $\xi_{s_3} = (0.001, 0.001, 0.8, 0.05, 0.5, 0.00001, 0.008, 3, 5, 0.96, 15, 2)'$ . The Nelder-Mead simplex algorithm delivers starting value independent results for the two-step estimation approach but not for the two other approaches. For them we employ the CMAES algorithm. The table also reports the values of the objective functions at the initial and the converged parameter values. The convergence criterion for the objective function is  $1 \cdot 10^{-15}$  and the convergence criterion for the parameters is  $1 \cdot 10^{-9}$ . A star indicates that the algorithm did not converge, given the maximum number of function evaluations, which was limited to  $3 \cdot 10^6$ .

|                          | Panel A              |                     |                     | Panel B             |                     |                     | Panel C             |                     |                     |
|--------------------------|----------------------|---------------------|---------------------|---------------------|---------------------|---------------------|---------------------|---------------------|---------------------|
|                          | $\xi_{s_1}^*$        | $\xi_{s_2}$         | $\xi_{s_3}^*$       | $\xi_{s_1}$         | $\xi_{s_2}$         | $\xi_{s_3}$         | $\xi_{s_1}$         | $\xi_{s_2}$         | $\xi_{s_3}$         |
| $\mu_c$                  | 0.0015               | 0.0010              | 0.0005              | 0.0015              | 0.0015              | 0.0003              | 0.0015              | 0.0015              | 0.0015              |
| $\mu_d$                  | 0.0017               | 0.0020              | 0.0005              | 0.0017              | 0.0017              | 0.0038              | 0.0017              | 0.0017              | 0.0017              |
| $\rho$                   | 0.9786               | 0.9618              | 0.8044              | 0.9994              | 0.9994              | 0.7287              | 0.9813              | 0.9813              | 0.9813              |
| $\varphi_e$              | 0.0454               | 0.0658              | 0.1324              | 0.0080              | 0.0076              | 0.1787              | 0.0426              | 0.0426              | 0.0426              |
| $\nu_1$                  | 0.9864               | 0.9645              | 0.7387              | 0.9873              | 0.9740              | 0.0336              |                     |                     |                     |
| $\sigma_w$               | $2.1 \cdot 10^{-6}$  | $1.1 \cdot 10^{-5}$ | $4.4 \cdot 10^{-6}$ | $2.0 \cdot 10^{-7}$ | $3.4 \cdot 10^{-9}$ | $4.2 \cdot 10^{-6}$ |                     |                     |                     |
| $\sigma$                 | 0.0078               | 0.0059              | 0.0117              | 0.0078              | 0.0078              | 0.0007              | 0.0078              | 0.0078              | 0.0078              |
| $\phi$                   | 2.9786               | 3.7873              | 6.0687              | 2.9254              | 2.9314              | 29.0190             | 2.6930              | 2.6930              | 2.6930              |
| $\varphi_d$              | 4.4856               | 2.6125              | 2.6915              | 4.4875              | 4.4962              | 53.1272             | 4.4919              | 4.4919              | 4.4919              |
| $\delta$                 | 0.9980               | 0.9975              | 0.9969              | 0.9977              | 0.9916              | 0.9911              | 0.9979              | 0.9979              | 0.9979              |
| $\gamma$                 | 10.1883              | 11.7574             | 14.7956             | 10.4576             | 9.1161              | 9.1177              | 10.4593             | 10.4593             | 10.4593             |
| $\psi$                   | 1.4974               | 2.1615              | 1.0517              | 0.9522              | 0.8443              | -0.0758             | 1.5677              | 1.5677              | 1.5677              |
| obj. fct.<br>(converged) | $4.4 \cdot 10^{-13}$ | $1.7 \cdot 10^{-6}$ | $7.2 \cdot 10^{-6}$ | $5.9 \cdot 10^{-6}$ | $5.9 \cdot 10^{-6}$ | $5.6 \cdot 10^{-4}$ | $1.1 \cdot 10^{-9}$ | $1.1 \cdot 10^{-9}$ | $1.1 \cdot 10^{-9}$ |
|                          |                      |                     |                     |                     |                     |                     | $3.4 \cdot 10^{-8}$ | $3.4 \cdot 10^{-8}$ | $3.4 \cdot 10^{-8}$ |
| obj. fct.<br>(initial)   | $3.3 \cdot 10^{-4}$  | 68.8180             | 395.0515            | $4.1 \cdot 10^{-5}$ | 0.0102              | 6.9203              | $2.7 \cdot 10^{-8}$ | $1.6 \cdot 10^{-7}$ | $8.3 \cdot 10^{-7}$ |
|                          |                      |                     |                     |                     |                     |                     | 0.3797              | 94.3059             | 398.5025            |

**Table 4: An analysis of moment sensitivity**

This table shows the sensitivity of the moments in Panel A of Table 1 to changes in the LRR model parameters. The moments are computed on the basis of a simulated sample size of  $5 \cdot 10^6$  observations, based on the parameter values from Table 2. The moment sensitivity in this table is computed as the relative change of a moment when one given parameter c.p. decreases by 50%. Each column of the table displays the sensitivity of all moments to a change of that size in the parameter given in the column header.

|   | $\mu_c$ | $\mu_d$ | $\rho$ | $\varphi_e$ | $\nu_1$ | $\sigma_w$ | $\sigma$ | $\phi$ | $\varphi_d$ | $\delta$ | $\gamma$ | $\psi$ |
|---|---------|---------|--------|-------------|---------|------------|----------|--------|-------------|----------|----------|--------|
| $\mathbb{E}(g)$                         | -0.50   | 0.00    | 0.00   | 0.00        | 0.00    | 0.00       | -0.00    | 0.00   | 0.00        | 0.00     | 0.00     | 0.00   |
| $\mathbb{E}(g_d)$                       | 0.00    | -0.50   | 0.00   | 0.00        | 0.00    | 0.00       | -0.00    | 0.00   | -0.00       | 0.00     | 0.00     | 0.00   |
| $\mathbb{E}(g^2)$                       | -0.03   | 0.00    | -0.04  | -0.03       | 0.00    | 0.00       | -0.67    | 0.00   | 0.00        | 0.00     | 0.00     | 0.00   |
| $\mathbb{E}(g_d^2)$                     | 0.00    | -0.00   | -0.02  | -0.02       | 0.00    | 0.00       | -0.69    | -0.02  | -0.73       | 0.00     | 0.00     | 0.00   |
| $\mathbb{E}(g_{t+1} \cdot g_t)$         | -0.34   | 0.00    | -0.53  | -0.41       | 0.00    | 0.00       | -0.39    | 0.00   | 0.00        | 0.00     | 0.00     | 0.00   |
| $\mathbb{E}(g_{t+2} \cdot g_t)$         | -0.34   | 0.00    | -0.53  | -0.41       | 0.00    | 0.00       | -0.38    | 0.00   | 0.00        | 0.00     | 0.00     | 0.00   |
| $\mathbb{E}(r_m - r_f)$                 | 0.01    | -0.03   | -1.18  | -0.86       | -0.04   | -0.03      | -0.66    | -0.69  | 0.12        | -1.18    | -0.69    | -0.38  |
| $\mathbb{E}(r_f)$                       | -0.23   | 0.00    | 0.17   | 0.13        | 0.01    | 0.01       | 0.27     | 0.00   | 0.00        | $> 10^2$ | 0.21     | 0.70   |
| $\mathbb{E}(z_m)$                       | 0.02    | -0.03   | 0.43   | 0.20        | 0.01    | 0.00       | 0.10     | 0.16   | -0.02       | -1.00    | 0.12     | -0.01  |
| $\mathbb{E}((r_m - r_f)^2)$             | 0.02    | -0.02   | -0.45  | -0.32       | -0.01   | -0.01      | -0.66    | -0.39  | -0.42       | -0.46    | 0.06     | -0.23  |
| $\mathbb{E}(r_f^2)$                     | -0.32   | 0.00    | 0.08   | 0.05        | 0.00    | 0.00       | 0.32     | 0.00   | 0.00        | $> 10^4$ | 0.36     | 2.12   |
| $\mathbb{E}(z_m^2)$                     | 0.04    | -0.05   | 1.06   | 0.43        | 0.01    | 0.01       | 0.21     | 0.34   | -0.04       | -1.00    | 0.25     | -0.02  |
| $\mathbb{E}(\xi^2)$                     | 0.00    | 0.00    | -0.04  | -0.03       | 0.00    | 0.00       | -0.70    | 0.00   | 0.00        | 0.00     | 0.00     | 0.00   |
| $\mathbb{E}(\xi_{t+1}^2 \cdot z_{m,t})$ | 0.02    | -0.03   | 0.38   | 0.16        | 0.01    | 0.01       | -0.67    | 0.16   | -0.02       | -1.00    | 0.12     | -0.01  |

**Table 5: Moment sensitivity to parameters for theory-based moments**

This table displays the sensitivity of the theory-based moments to changes in the preference parameters using the simulated part of the moment match. The moments are computed from a simulated sample of size of  $10^6$  observations, based on the parameters from Table 2. The moment sensitivity in this table is computed as the relative change of a moment when one given parameter c.p. decreases by 10%. Each column of the table displays the sensitivity of all moments to a change of that size in the parameter given in the column header.

|  | $\delta$ | $\gamma$ | $\psi$ |
|--|----------|----------|--------|
| $\mathbb{E}(M)$  | -0.10    | -0.00    | -0.00  |
| $\frac{-\text{Cov}(R_m - R_f, M)}{\mathbb{E}(M)}$        | -0.97    | -0.10    | -0.04  |
| $\mathbb{E}[(R_m - R_f)^2]$                              | -0.32    | 0.01     | -0.03  |
| $\frac{\text{Cov}(R_{f,t+1}, z_{m,t})}{\text{Var}(z_m)}$ | 4.28     | -0.01    | 0.14   |
| $\mathbb{E}(z_m)$  | -0.60    | 0.02     | -0.00  |
| $\mathbb{E}(z_m^2)$                                      | -0.84    | 0.04     | -0.00  |

**Table 6: Moment matches used for GMM estimation of macro parameters**

For GMM estimation of  $\xi_{M^*}$ , the basic set of first and second moment conditions in Equation (34) is always included. The maximum lag lengths of the (cross-) auto-moments in Equation (35) vary according to the scheme below.

| moment set    | $L_1$ | $L_2$ | $L_3$ |
|---------------|-------|-------|-------|
| <b>7 mc</b>   | 2     | 0     | 0     |
| <b>15 mc</b>  | 5     | 5     | 0     |
| <b>20 mc</b>  | 5     | 5     | 5     |
| <b>35 mc</b>  | 10    | 10    | 10    |
| <b>87 mc</b>  | 36    | 36    | 10    |
| <b>113 mc</b> | 36    | 36    | 36    |
| <b>149 mc</b> | 48    | 48    | 48    |
| <b>185 mc</b> | 60    | 60    | 60    |

**Table 7: Means and standard deviations of GMM estimates  $\hat{\mu}_c$  and  $\hat{\mu}_d$** 

This table reports the means and the standard deviations of the GMM parameter estimates  $\hat{\mu}_c$  and  $\hat{\mu}_d$ . For each sample size  $T$ , 400 data sets were simulated and the estimation was performed using 8 different moment sets, ranging from 7 to 185 moment conditions (cf. Table 6).

|                                  | 7mc                    | 15mc                   | 20mc                   | 35mc                   | 87mc                   | 113mc                  | 149mc                  | 185mc                  |
|----------------------------------|------------------------|------------------------|------------------------|------------------------|------------------------|------------------------|------------------------|------------------------|
| <b><math>\mu_c=0.0015</math></b> |                        |                        |                        |                        |                        |                        |                        |                        |
| <b>T=1000</b>                    | 0.001588<br>(0.000501) | 0.001557<br>(0.000529) | 0.001566<br>(0.000548) | 0.001539<br>(0.000556) | 0.001549<br>(0.000536) | 0.001557<br>(0.000534) | 0.001552<br>(0.000525) | 0.001566<br>(0.000520) |
| <b>T=2000</b>                    | 0.001546<br>(0.000359) | 0.001530<br>(0.000381) | 0.001529<br>(0.000378) | 0.001532<br>(0.000371) | 0.001531<br>(0.000366) | 0.001521<br>(0.000368) | 0.001524<br>(0.000373) | 0.001524<br>(0.000367) |
| <b>T=5000</b>                    | 0.001522<br>(0.000239) | 0.001523<br>(0.000240) | 0.001529<br>(0.000237) | 0.001524<br>(0.000237) | 0.001519<br>(0.000243) | 0.001517<br>(0.000242) | 0.001519<br>(0.000242) | 0.001522<br>(0.000238) |
| <b>T=100,000</b>                 | 0.001496<br>(0.000058) | 0.001495<br>(0.000058) | 0.001496<br>(0.000058) | 0.001496<br>(0.000059) | 0.001496<br>(0.000059) | 0.001496<br>(0.000059) | 0.001496<br>(0.000059) | 0.001496<br>(0.000059) |
| <b><math>\mu_d=0.0015</math></b> |                        |                        |                        |                        |                        |                        |                        |                        |
| <b>T=1000</b>                    | 0.002084<br>(0.001446) | 0.001948<br>(0.001559) | 0.002033<br>(0.001604) | 0.002012<br>(0.001602) | 0.001949<br>(0.001485) | 0.001982<br>(0.001505) | 0.001947<br>(0.001486) | 0.002017<br>(0.001467) |
| <b>T=2000</b>                    | 0.001749<br>(0.001124) | 0.001661<br>(0.001172) | 0.001685<br>(0.001190) | 0.001730<br>(0.001179) | 0.001677<br>(0.001153) | 0.001651<br>(0.001139) | 0.001669<br>(0.001158) | 0.001665<br>(0.001149) |
| <b>T=5000</b>                    | 0.001590<br>(0.000816) | 0.001601<br>(0.000804) | 0.001616<br>(0.000801) | 0.001604<br>(0.000805) | 0.001574<br>(0.000832) | 0.001576<br>(0.000836) | 0.001577<br>(0.000835) | 0.001589<br>(0.000830) |
| <b>T=100,000</b>                 | 0.001482<br>(0.000191) | 0.001481<br>(0.000192) | 0.001481<br>(0.000192) | 0.001481<br>(0.000192) | 0.001482<br>(0.000192) | 0.001482<br>(0.000192) | 0.001482<br>(0.000192) | 0.001482<br>(0.000192) |

**Table 8: Means and standard deviations of GMM estimates  $\hat{\rho}$  and  $\hat{\varphi}_e$**   
 This table reports the means and the standard deviations of the GMM parameter estimates  $\hat{\rho}$  and  $\hat{\varphi}_e$ . For each sample size  $T$ , 400 data sets were simulated and the estimation was performed using 8 different moment sets, ranging from 7 to 185 moment conditions (cf. Table 6).

|                                      | 7mc                    | 15mc                   | 20mc                   | 35mc                   | 87mc                   | 113mc                  | 149mc                  | 185mc                  |
|--------------------------------------|------------------------|------------------------|------------------------|------------------------|------------------------|------------------------|------------------------|------------------------|
| <b><math>\rho=0.9790</math></b>      |                        |                        |                        |                        |                        |                        |                        |                        |
| <b>T=1000</b>                        | 0.808712<br>(0.293789) | 0.751218<br>(0.325286) | 0.788771<br>(0.290278) | 0.803248<br>(0.292826) | 0.917071<br>(0.156420) | 0.926602<br>(0.150617) | 0.925134<br>(0.145199) | 0.914304<br>(0.170581) |
| <b>T=2000</b>                        | 0.843687<br>(0.238097) | 0.803634<br>(0.259096) | 0.807005<br>(0.274239) | 0.837530<br>(0.263833) | 0.949981<br>(0.103534) | 0.954998<br>(0.095277) | 0.952202<br>(0.107220) | 0.954707<br>(0.087877) |
| <b>T=5000</b>                        | 0.890665<br>(0.155095) | 0.879996<br>(0.181472) | 0.898257<br>(0.148819) | 0.933842<br>(0.121116) | 0.971759<br>(0.049922) | 0.972920<br>(0.047260) | 0.972324<br>(0.047247) | 0.972734<br>(0.027517) |
| <b>T=100,000</b>                     | 0.931789<br>(0.099321) | 0.969324<br>(0.033394) | 0.971714<br>(0.030141) | 0.977699<br>(0.015070) | 0.978944<br>(0.004005) | 0.978968<br>(0.003863) | 0.978865<br>(0.003003) | 0.978726<br>(0.002683) |
| <b><math>\varphi_e=0.0440</math></b> |                        |                        |                        |                        |                        |                        |                        |                        |
| <b>T=1000</b>                        | 0.075223<br>(0.099367) | 0.065644<br>(0.089732) | 0.071262<br>(0.088866) | 0.068932<br>(0.081661) | 0.053135<br>(0.055733) | 0.052875<br>(0.054500) | 0.056154<br>(0.051267) | 0.056177<br>(0.047299) |
| <b>T=2000</b>                        | 0.079019<br>(0.090658) | 0.065668<br>(0.074406) | 0.071638<br>(0.080417) | 0.068225<br>(0.072669) | 0.046782<br>(0.043367) | 0.045572<br>(0.042948) | 0.050383<br>(0.044188) | 0.053195<br>(0.044524) |
| <b>T=5000</b>                        | 0.080681<br>(0.081350) | 0.054945<br>(0.059491) | 0.062062<br>(0.066043) | 0.055617<br>(0.053241) | 0.042828<br>(0.039532) | 0.043298<br>(0.034905) | 0.045803<br>(0.033780) | 0.047415<br>(0.028952) |
| <b>T=100,000</b>                     | 0.062456<br>(0.052848) | 0.040432<br>(0.034373) | 0.040156<br>(0.034101) | 0.041713<br>(0.020359) | 0.043773<br>(0.004770) | 0.043746<br>(0.005509) | 0.043974<br>(0.004320) | 0.044204<br>(0.004015) |



**Table 9: Means and standard deviations of GMM estimates  $\hat{\sigma}$  and  $\hat{\phi}$**

This table reports the means and the standard deviations of the GMM parameter estimates  $\hat{\sigma}$  and  $\hat{\phi}$ . For each sample size  $T$ , 400 data sets were simulated and the estimation was performed using 8 different moment sets, ranging from 7 to 185 moment conditions (cf. Table 6).

|                                   | <b>7mc</b>             | <b>15mc</b>            | <b>20mc</b>            | <b>35mc</b>            | <b>87mc</b>            | <b>113mc</b>           | <b>149mc</b>           | <b>185mc</b>           |
|-----------------------------------|------------------------|------------------------|------------------------|------------------------|------------------------|------------------------|------------------------|------------------------|
| <b><math>\sigma=0.0078</math></b> |                        |                        |                        |                        |                        |                        |                        |                        |
| <b>T=1000</b>                     | 0.007772<br>(0.000412) | 0.007791<br>(0.000431) | 0.007799<br>(0.000410) | 0.007775<br>(0.000464) | 0.007789<br>(0.000404) | 0.007770<br>(0.000459) | 0.007784<br>(0.000411) | 0.007778<br>(0.000404) |
| <b>T=2000</b>                     | 0.007788<br>(0.000296) | 0.007824<br>(0.000284) | 0.007804<br>(0.000296) | 0.007766<br>(0.000493) | 0.007799<br>(0.000356) | 0.007798<br>(0.000331) | 0.007790<br>(0.000355) | 0.007781<br>(0.000384) |
| <b>T=5000</b>                     | 0.007785<br>(0.000198) | 0.007834<br>(0.000182) | 0.007800<br>(0.000187) | 0.007779<br>(0.000386) | 0.007814<br>(0.000184) | 0.007818<br>(0.000177) | 0.007814<br>(0.000179) | 0.007815<br>(0.000179) |
| <b>T=100,000</b>                  | 0.007791<br>(0.000048) | 0.007803<br>(0.000043) | 0.007800<br>(0.000044) | 0.007801<br>(0.000043) | 0.007803<br>(0.000041) | 0.007803<br>(0.000042) | 0.007803<br>(0.000042) | 0.007802<br>(0.000042) |
| <b><math>\phi=3.0</math></b>      |                        |                        |                        |                        |                        |                        |                        |                        |
| <b>T=1000</b>                     | 4.079648<br>(5.334688) | 5.322702<br>(5.634923) | 5.377577<br>(5.253479) | 5.060300<br>(5.231113) | 4.193287<br>(4.212258) | 3.875414<br>(3.460940) | 4.036691<br>(3.689799) | 4.118246<br>(3.976272) |
| <b>T=2000</b>                     | 3.878558<br>(4.334499) | 5.367465<br>(4.839307) | 5.066246<br>(4.745072) | 4.353708<br>(4.097956) | 3.594153<br>(2.747727) | 3.436140<br>(2.523522) | 3.307435<br>(1.996180) | 3.357487<br>(1.942996) |
| <b>T=5000</b>                     | 2.983722<br>(2.576938) | 4.753321<br>(4.281023) | 3.837608<br>(2.570627) | 3.372612<br>(1.651467) | 3.116605<br>(0.905312) | 3.095433<br>(0.828071) | 3.104853<br>(0.823260) | 3.111128<br>(0.759768) |
| <b>T=100,000</b>                  | 2.973181<br>(1.616907) | 3.116188<br>(0.934635) | 3.038033<br>(0.290304) | 3.011684<br>(0.190327) | 3.010016<br>(0.148244) | 3.012849<br>(0.144897) | 3.012190<br>(0.142191) | 3.010695<br>(0.142076) |

**Table 10: Means and standard deviations of GMM estimates  $\hat{\varphi}_d$** 

This table reports the means and the standard deviations of the GMM parameter estimate  $\hat{\varphi}_d$ . For each sample size  $T$ , 400 data sets were simulated and the estimation was performed using 8 different moment sets, ranging from 7 to 185 moment conditions (cf. Table 6).

|                  | <b>7mc</b>             | <b>15mc</b>            | <b>20mc</b>            | <b>35mc</b>            | <b>87mc</b>            | <b>113mc</b>           | <b>149mc</b>           | <b>185mc</b>           |
|------------------|------------------------|------------------------|------------------------|------------------------|------------------------|------------------------|------------------------|------------------------|
| $\varphi_d=4.5$  |                        |                        |                        |                        |                        |                        |                        |                        |
| <b>T=1000</b>    | 4.442414<br>(0.272011) | 4.470252<br>(0.200707) | 4.461027<br>(0.198498) | 4.494593<br>(0.297396) | 4.491056<br>(0.174139) | 4.495483<br>(0.251202) | 4.483134<br>(0.167098) | 4.489017<br>(0.168620) |
| <b>T=2000</b>    | 4.468676<br>(0.192713) | 4.448006<br>(0.160857) | 4.464787<br>(0.165845) | 4.581143<br>(1.643127) | 4.503892<br>(0.321805) | 4.503805<br>(0.221512) | 4.509860<br>(0.284563) | 4.516286<br>(0.332658) |
| <b>T=5000</b>    | 4.504565<br>(0.116551) | 4.461806<br>(0.121951) | 4.486654<br>(0.101916) | 4.561332<br>(1.214736) | 4.495095<br>(0.077883) | 4.493135<br>(0.072184) | 4.495772<br>(0.072824) | 4.495031<br>(0.073611) |
| <b>T=100,000</b> | 4.505292<br>(0.044705) | 4.496131<br>(0.020153) | 4.498794<br>(0.019967) | 4.498771<br>(0.018085) | 4.498175<br>(0.016623) | 4.498054<br>(0.016878) | 4.498214<br>(0.016946) | 4.498434<br>(0.016911) |

**Table 11: Moment matches selected by GMM-BIC**

This table displays the number of replications in which a given moment set minimizes the BIC criterion for each  $T$ . Replications with implausible parameter estimates, failed computations of the GMM-BIC, or for which the optimization algorithm did not converge were dropped. We consider an estimate implausible if it is ten times bigger than the true parameter value. Furthermore, we discarded any replication for which the J-statistic lies above the 99.999% quantile of the respective  $\chi^2$  distribution, which leads to an implausibly high value of the GMM-BIC.

|                  | <b>7mc</b> | <b>15mc</b> | <b>20mc</b> | <b>35mc</b> | <b>87mc</b> | <b>113mc</b> | <b>149mc</b> | <b>185mc</b> |
|------------------|------------|-------------|-------------|-------------|-------------|--------------|--------------|--------------|
| <b>T=1000</b>    | 0          | 1           | 5           | 12          | 11          | 13           | 31           | 255          |
| <b>T=2000</b>    | 0          | 1           | 2           | 6           | 1           | 12           | 25           | 308          |
| <b>T=5000</b>    | 0          | 1           | 0           | 0           | 0           | 3            | 24           | 364          |
| <b>T=100,000</b> | 0          | 0           | 0           | 0           | 0           | 0            | 0            | 400          |

**Table 12: Successful estimations for the macro parameters**

The table reports the number of successful first-step estimations for each sample size  $T$ . The total number of replications is 400. The results of any replication are dropped if one of the parameter estimates is greater than ten times the true value or if the optimization algorithm did not converge.

|                  | <b>7mc</b> | <b>15mc</b> | <b>20mc</b> | <b>35mc</b> | <b>87mc</b> | <b>113mc</b> | <b>149mc</b> | <b>185mc</b> |
|------------------|------------|-------------|-------------|-------------|-------------|--------------|--------------|--------------|
| <b>T=1000</b>    | 248        | 227         | 257         | 281         | 317         | 326          | 325          | 321          |
| <b>T=2000</b>    | 325        | 267         | 317         | 324         | 355         | 363          | 358          | 365          |
| <b>T=5000</b>    | 375        | 341         | 360         | 369         | 392         | 393          | 394          | 389          |
| <b>T=100,000</b> | 397        | 394         | 397         | 399         | 400         | 399          | 399          | 400          |

**Table 13: Means and standard deviations of the SMM estimates  $\hat{\delta}$ ,  $\hat{\gamma}$ , and  $\hat{\psi}$**   
 Panel A reports the means and standard deviations of the preference parameter SMM estimates that use the true macro parameters for the moment simulation. The first column of Panel A reports the results based on the ad hoc moment matches in Panel A-2 of Table 1, the second column reports the results for the theory-based moment matches  $\mathbf{G}_T^P = (\mathbf{G}_T^{P_1}, \mathbf{G}_T^{P_2}, \mathbf{G}_T^{P_3}, \mathbf{G}_T^{P_4})'$ . In both cases, SMM estimates are obtained by concentrating out stochastic volatility, i.e. using  $\sigma = \mathbb{E}(\sigma_t^2)$  for SMM. The third column of Panel A contains the SMM estimation results assuming the complete vector of macro parameters as known, and thus using  $\sigma_t^2$  when simulating the theory-based financial moments. Panel B reports the means and standard deviations of the SMM preference parameter estimates that use the estimated macro parameters for the simulation of moments.

|                                   | Panel A               |                     |                     | Panel B                    |                      |
|-----------------------------------|-----------------------|---------------------|---------------------|----------------------------|----------------------|
|                                   | true macro parameters |                     |                     | estimated macro parameters |                      |
|                                   | ad hoc                | theory-based        | + SV known          | ad hoc                     | theory-based         |
| <b><math>\delta=0.9980</math></b> |                       |                     |                     |                            |                      |
| <b>T=1000</b>                     | 0.9981<br>(0.0008)    | 0.9980<br>(0.0006)  | 0.9981<br>(0.0006)  | 0.9955<br>(0.0047)         | 0.9965<br>(0.0021)   |
| <b>T=2000</b>                     | 0.9980<br>(0.0006)    | 0.9980<br>(0.0004)  | 0.9980<br>(0.0004)  | 0.9966<br>(0.0027)         | 0.9972<br>(0.0019)   |
| <b>T=5000</b>                     | 0.9979<br>(0.0004)    | 0.9980<br>(0.0003)  | 0.9980<br>(0.0003)  | 0.9979<br>(0.0011)         | 0.9978<br>(0.0007)   |
| <b>T=100,000</b>                  | 0.9979<br>(0.0002)    | 0.9980<br>(0.0001)  | 0.9980<br>(0.0001)  | 0.9980<br>(0.0005)         | 0.9980<br>(0.0002)   |
| <b><math>\gamma=10</math></b>     |                       |                     |                     |                            |                      |
| <b>T=1000</b>                     | 10.5409<br>(1.4146)   | 10.3399<br>(1.1108) | 10.0748<br>(0.9604) | 34.4836<br>(82.5210)       | 26.5381<br>(28.4748) |
| <b>T=2000</b>                     | 10.3125<br>(1.0566)   | 10.2983<br>(0.7999) | 10.0230<br>(0.7151) | 19.5936<br>(38.9336)       | 16.4719<br>(14.8120) |
| <b>T=5000</b>                     | 10.2542<br>(0.7275)   | 10.3380<br>(0.5097) | 10.0145<br>(0.4542) | 11.7276<br>(6.9328)        | 12.7821<br>(5.7417)  |
| <b>T=100,000</b>                  | 10.1376<br>(0.3114)   | 10.3287<br>(0.1112) | 9.9986<br>(0.0968)  | 10.3326<br>(0.6271)        | 10.3929<br>(0.6996)  |
| <b><math>\psi=1.5</math></b>      |                       |                     |                     |                            |                      |
| <b>T=1000</b>                     | 1.8402<br>(1.7972)    | 1.5171<br>(0.0542)  | 1.4946<br>(0.0560)  | 4.0093<br>(9.5282)         | 3.1949<br>(3.6131)   |
| <b>T=2000</b>                     | 1.9827<br>(4.9717)    | 1.5149<br>(0.0256)  | 1.4981<br>(0.0308)  | 3.3048<br>(5.4362)         | 2.5063<br>(1.8937)   |
| <b>T=5000</b>                     | 1.7570<br>(1.3764)    | 1.5154<br>(0.0428)  | 1.5003<br>(0.0353)  | 3.2752<br>(7.4588)         | 1.9462<br>(1.5177)   |
| <b>T=100,000</b>                  | 1.7964<br>(2.2075)    | 1.5129<br>(0.0017)  | 1.4999<br>(0.0020)  | 1.7586<br>(0.9212)         | 1.5279<br>(0.1533)   |

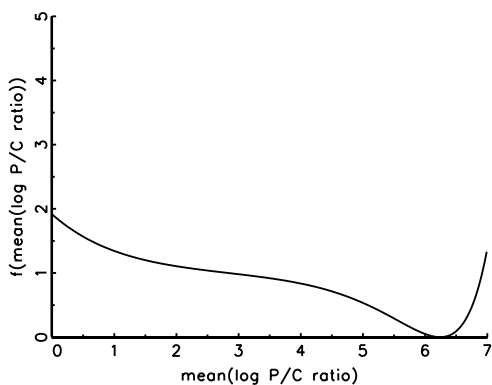
**Table 14: Means and standard deviations of the preference parameter estimates using an efficient weighting matrix estimate in the first step and pre-selecting first-step results**

Panel A shows the SMM estimation results for the preference parameters that are based on the “efficient” macro parameter estimates. These estimates are obtained by a two-stage GMM procedure. The first stage uses  $\mathbf{W}_T^M = \mathbf{I}$  in Equation (31) to get an initial estimate  $\xi_{M^*}$ , which is then used to compute an estimate of the efficient GMM weighting matrix  $\mathbf{W}_e^M$ . Second-stage GMM estimates of  $\xi_{M^*}$  result from using  $\mathbf{W}_T^M = \widehat{\mathbf{W}}_e^M$  in Equation (31). Panel B reveals the incremental effect of raising the bar for the quality of the first-step GMM estimates before allowing to enter the SMM step. For that purpose we discard any replication for which one of the macro parameter estimates is more than twice its true value.

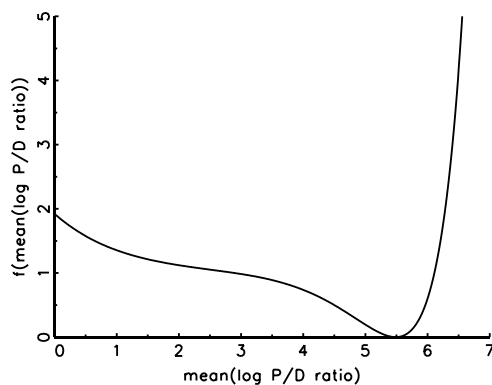
|                                   | <b>Panel A</b>       | <b>Panel B</b>      |
|-----------------------------------|----------------------|---------------------|
|                                   | eff. GMM             | eff. GMM + select.  |
| <hr/>                             |                      |                     |
| <b><math>\delta=0.9980</math></b> |                      |                     |
| <b>T=1000</b>                     | 0.9970<br>(0.0024)   | 0.9971<br>(0.0016)  |
| <b>T=2000</b>                     | 0.9974<br>(0.0013)   | 0.9975<br>(0.0012)  |
| <b>T=5000</b>                     | 0.9978<br>(0.0007)   | 0.9978<br>(0.0006)  |
| <b>T=100,000</b>                  | 0.9980<br>(0.0001)   | 0.9980<br>(0.0001)  |
| <hr/>                             |                      |                     |
| <b><math>\gamma=10</math></b>     |                      |                     |
| <b>T=1000</b>                     | 19.8183<br>(23.9993) | 15.2541<br>(9.7201) |
| <b>T=2000</b>                     | 14.5322<br>(14.4060) | 12.9144<br>(9.4942) |
| <b>T=5000</b>                     | 12.0499<br>(4.7351)  | 11.9741<br>(4.5265) |
| <b>T=100,000</b>                  | 10.3809<br>(0.6776)  | 10.3809<br>(0.6776) |
| <hr/>                             |                      |                     |
| <b><math>\psi=1.5</math></b>      |                      |                     |
| <b>T=1000</b>                     | 2.8801<br>(2.9754)   | 2.1014<br>(1.1945)  |
| <b>T=2000</b>                     | 2.1048<br>(1.4821)   | 1.9226<br>(1.0531)  |
| <b>T=5000</b>                     | 1.7309<br>(0.6011)   | 1.7105<br>(0.4665)  |
| <b>T=100,000</b>                  | 1.5248<br>(0.0976)   | 1.5248<br>(0.0976)  |
| <hr/>                             |                      |                     |

**Figure 1: (Non-) existence of the solution for the endogenous LRR model parameters**

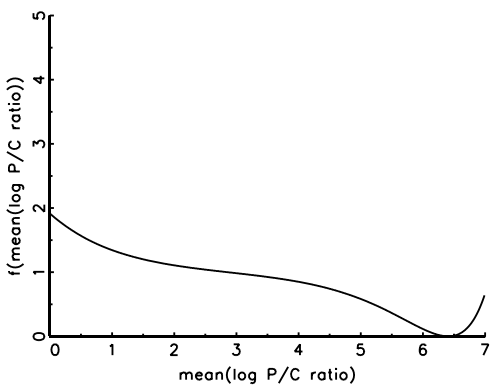
Solving for the endogenous parameters amounts to finding the roots of the squared deviations between the hypothesized means of the log price-consumption ratio ( $\bar{z}$ ) and the log price-dividend ratio ( $\bar{z}_m$ ) and the model-implied means. If the deviation functions do not both have a root, the LRR model cannot be solved. The upper panels show a plot of these two deviation functions based on the LRR parameter values chosen by [Bansal and Yaron \(2004\)](#) for their calibration of the LRR model (see [Table 2](#)). The lower panels show that a change of these parameters within a plausible range may yield an unsolvable model: changing the value of the risk aversion parameter from  $\gamma = 10$  to  $\gamma = 4$  and the mean of dividend growth from  $\mu_d = 0.0015$  to  $\mu_d = 0.0035$ , leaving all other parameters unchanged, implies that one of the two functions does not have a root.



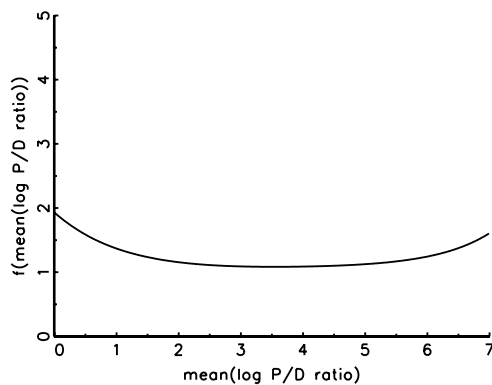
root  $\bar{z}^*$  exists for  $\gamma = 10, \mu_d = 0.0015$



root  $\bar{z}_m^*$  exists for  $\gamma = 10, \mu_d = 0.0015$



root  $\bar{z}^*$  exists for  $\gamma = 4, \mu_d = 0.0035$



no root  $\bar{z}_m^*$  exists for  $\gamma = 4, \mu_d = 0.0035$

**Figure 2: Autocorrelograms of simulated consumption and dividend growth**

These autocorrelograms illustrate the persistence of the growth processes defining the macroeconomy. The graphs are based on a model simulation with the parameter values used by [Bansal and Yaron \(2004\)](#), as listed in [Table 2](#), and a simulated sample size of  $\mathcal{T}(T) = 10^6$  observations. The abscissa spans a time interval of 10 years, and the half-life of both autocorrelations is about three years.

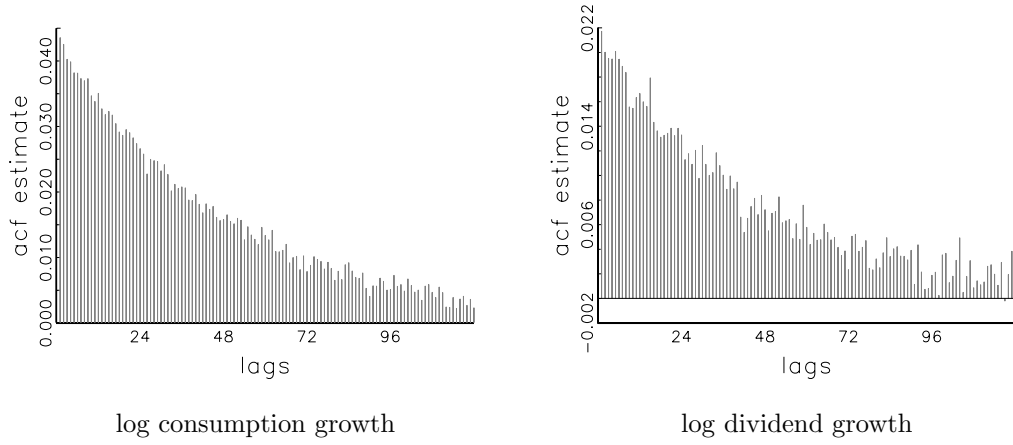


**Figure 3: Kernel densities for  $\hat{\mu}_c$ ,  $\hat{\mu}_d$ ,  $\hat{\sigma}$ , and  $\hat{\varphi}_d$**

The figure displays the kernel densities for the macro parameters that prove less difficult to estimate and that result from using alternative moment matches (cf. Table 6). To account for the boundedness of the parameters, we use the beta kernel proposed by [Chen \(1999\)](#) with the bandwidth selector by [Silverman \(1986\)](#), adjusted for variable kernels. The vertical lines indicate the positions of the true parameters.

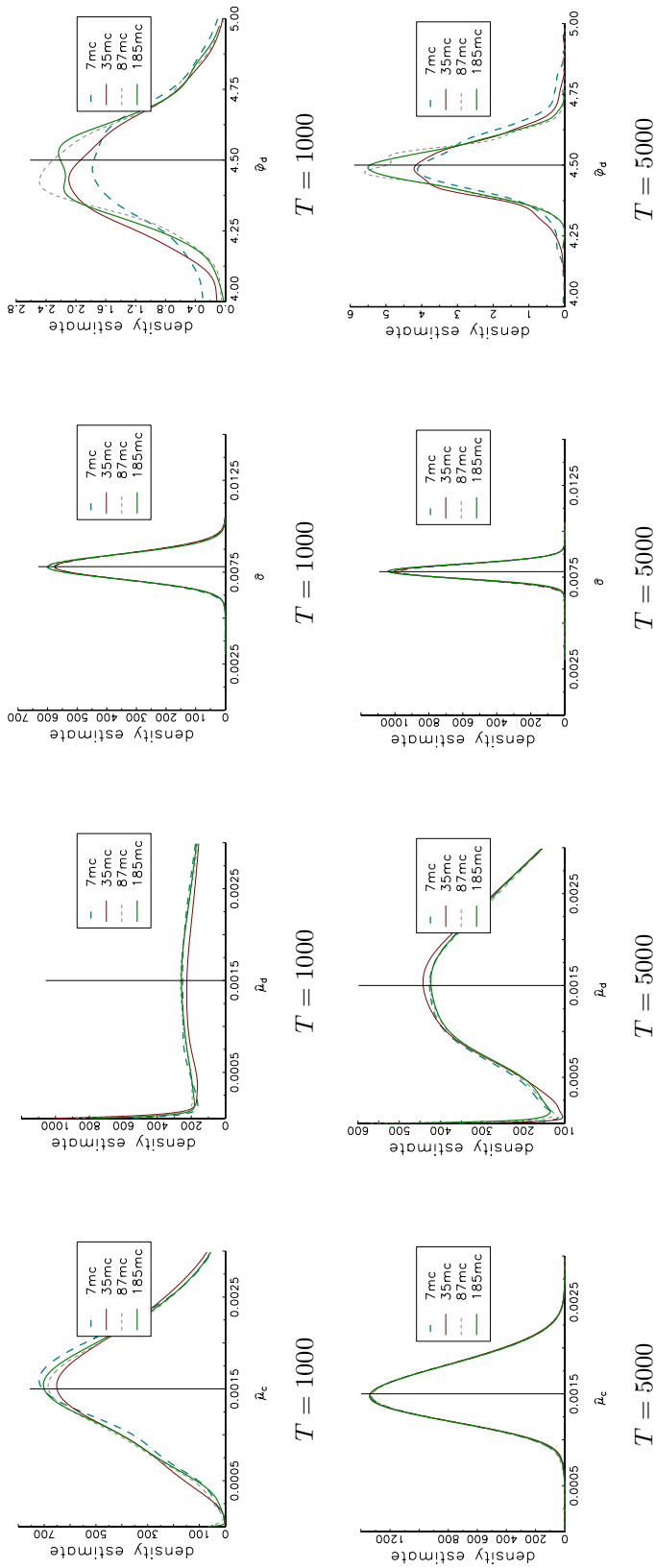




**Figure 4: Kernel densities for  $\hat{\rho}$ ,  $\hat{\varphi}_e$ , and  $\hat{\phi}$**

The figure displays the kernel densities for the critical macro parameters that result from different moment matches (cf. Table 6). To account for the boundedness of the parameters, we use the beta kernel proposed by [Chen \(1999\)](#) with the bandwidth selector by [Silverman \(1986\)](#), adjusted for variable kernels. The vertical lines indicate the positions of the true parameters.

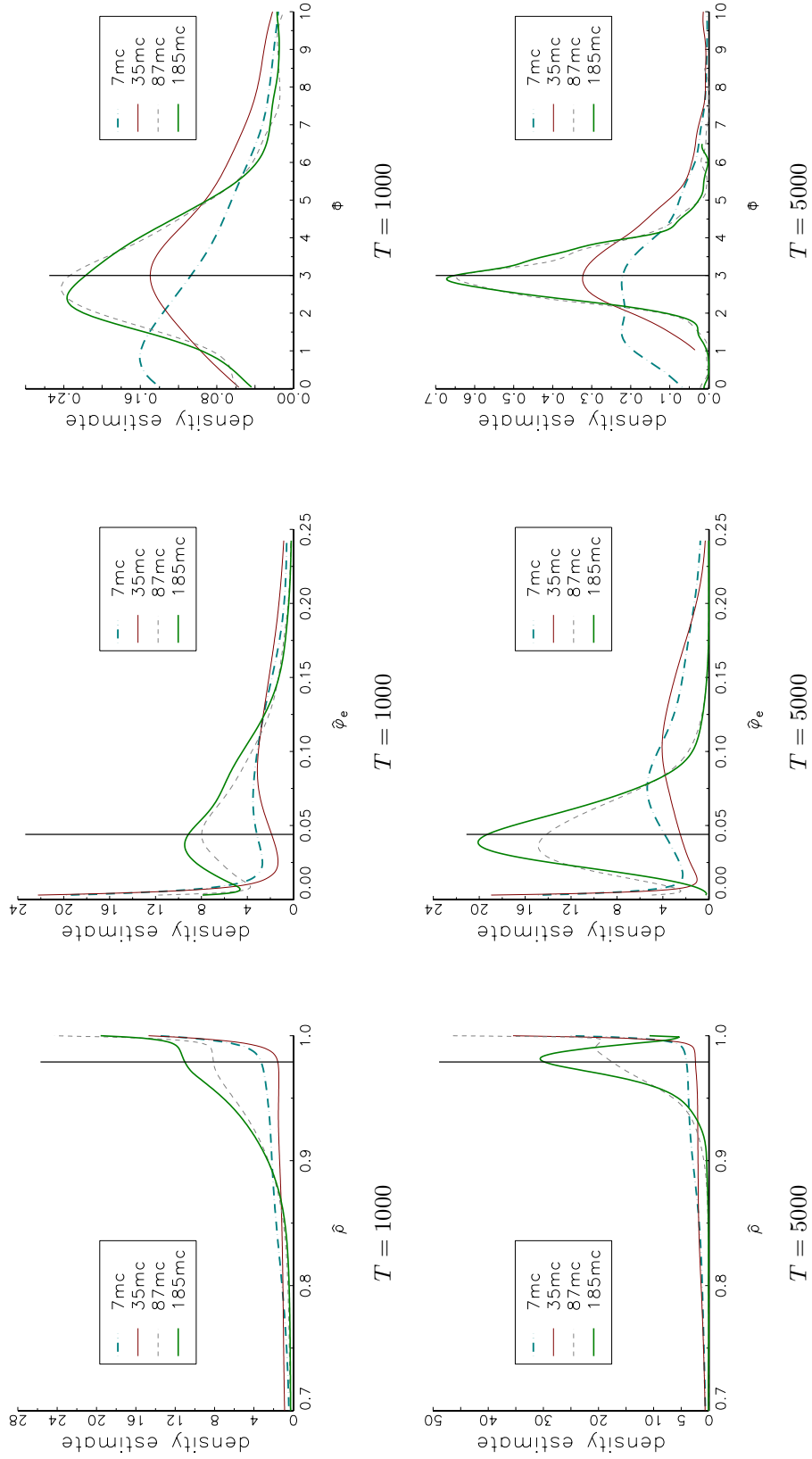


**Figure 5: Kernel densities for  $\hat{\delta}$ ,  $\hat{\gamma}$ , and  $\hat{\psi}$**

The figure displays kernel density estimates for the preference parameter estimates resulting from using theory-based (red solid line) and ad hoc (blue dashes) financial moment matches. SMM is based on the knowledge of the true macro parameters; SV is concentrated out when simulating moments. The vertical lines indicate the positions of the true parameters. The Gaussian kernel with bandwidth as proposed by [Silverman \(1986\)](#) is employed.

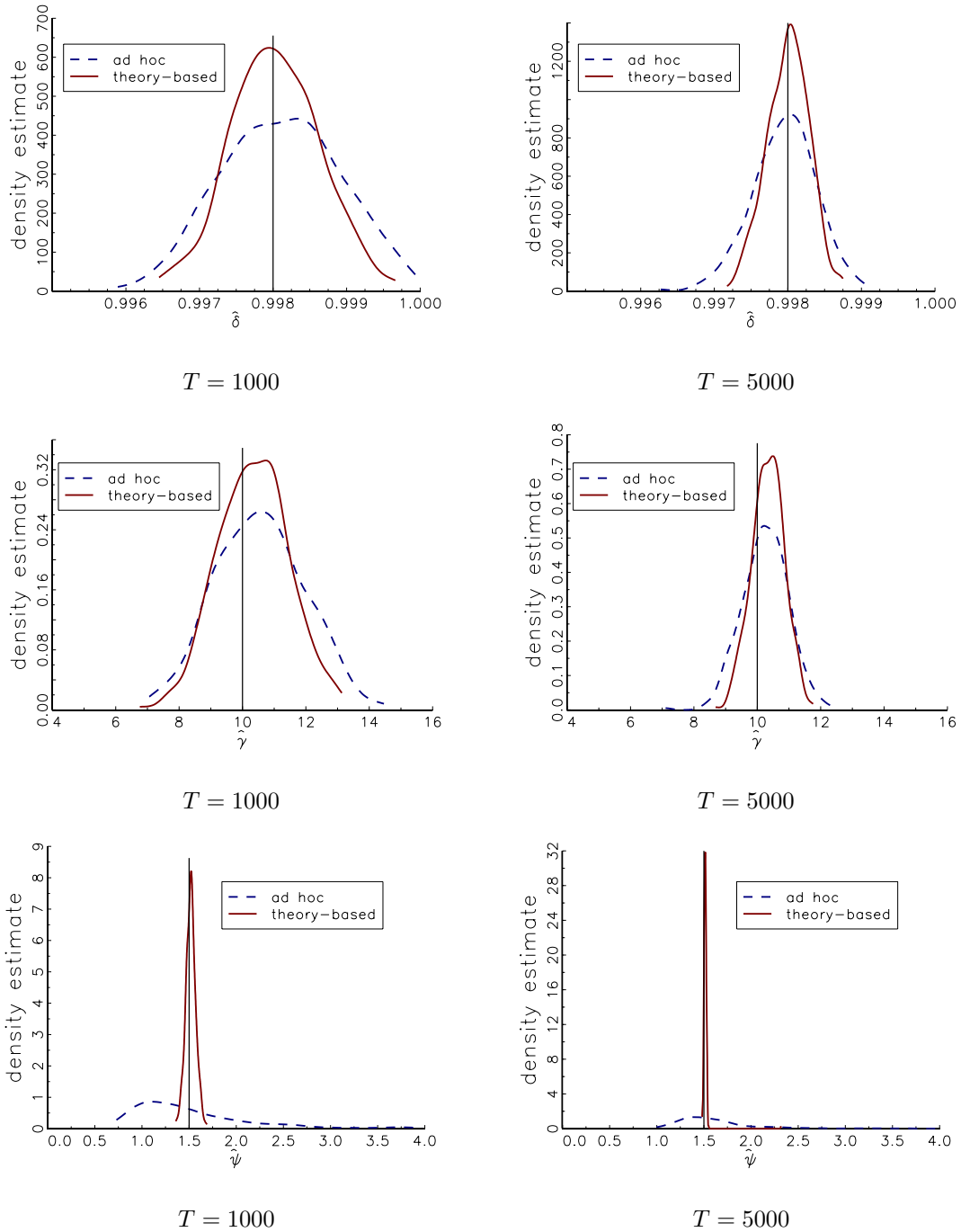
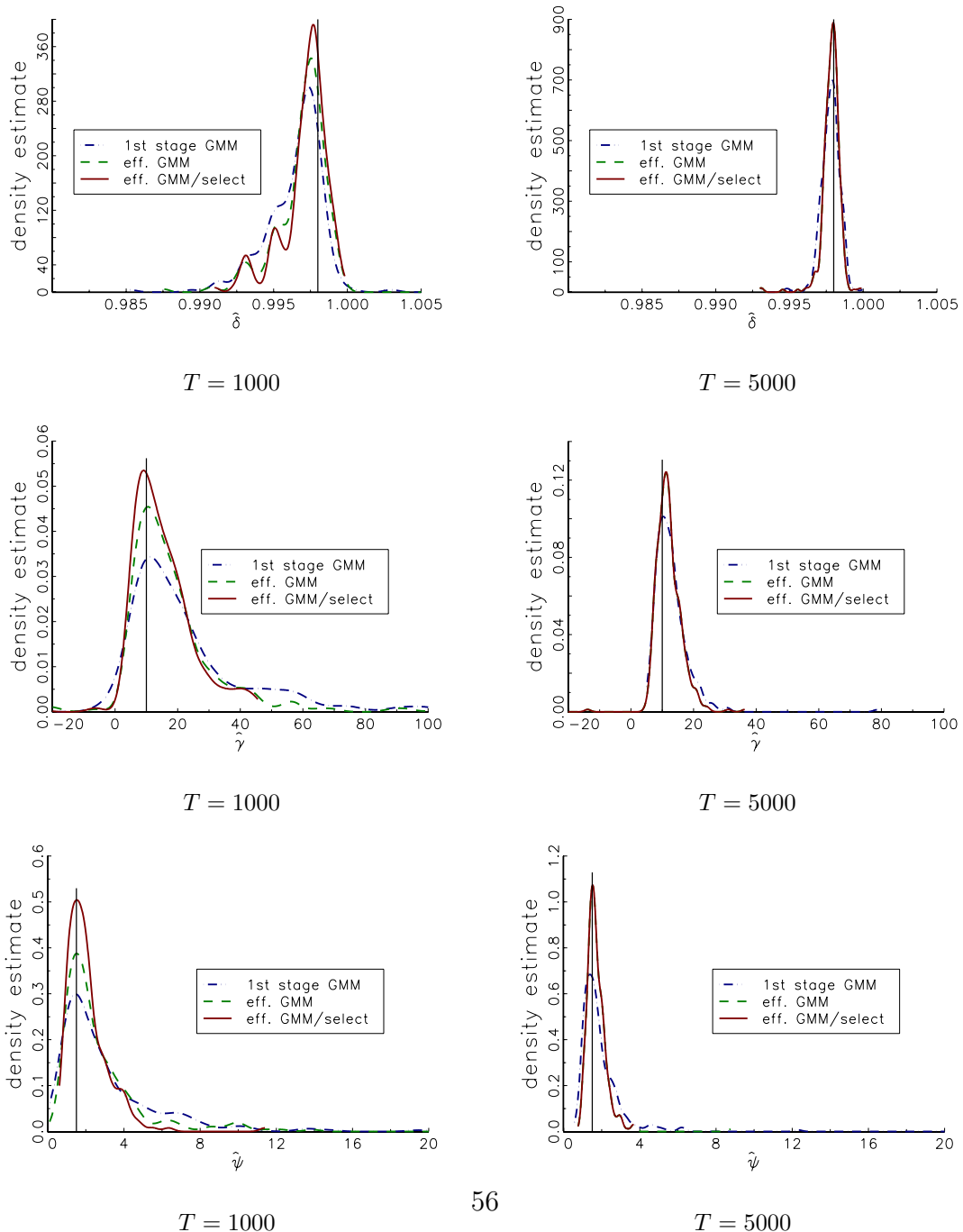


**Figure 6: Kernel densities for  $\hat{\delta}$ ,  $\hat{\gamma}$ , and  $\hat{\psi}$**

The figure displays three kernel density estimates for preference parameter estimates that result from using estimated macro parameters and theory-based financial moment matches. The first (blue dashes-dots) uses first-step macro GMM estimates based on the 185 mc moment set and an identity weighting matrix for GMM (1st stage GMM). The second (green dashes) instead uses an estimate of the efficient GMM weighting matrix (eff. GMM) when estimating the macro parameters. The third (red solid line) also uses efficient weighting but additionally applies a more restrictive selection criterion in that the second-step SMM estimation of the preference parameters is not performed if one of the first-step macro estimates is twice as large as the true parameter value (eff. GMM/select). The vertical lines indicate the positions of the true parameters. The Gaussian kernel with bandwidth as proposed by [Silverman \(1986\)](#) is employed.



## Recent Issues

All CFS Working Papers are available at [www.ifk-cfs.de](http://www.ifk-cfs.de).

| No. | Authors   | Title   |
|-----|---|---|
| 478 | Anders Warne, Günter Coenen, Kai Christoffel                            | <i>Marginalized Predictive Likelihood Comparisons of Linear Gaussian State-Space Models with Applications to DSGE, DSGE-VAR, and VAR Models</i> |
| 477 | Markus Bibinger, Nikolaus Hautsch, Peter Malec, Markus Reiss            | <i>Estimating the Spot Covariation of Asset Prices – Statistical Theory and Empirical Evidence</i>  |
| 476 | Christina Bannier, Markus Wiemann                                       | <i>Performance-Sensitive Debt – the Intertwined Effects of Performance Measurement and Pricing Grid Asymmetry</i>                               |
| 475 | Christina Bannier, Eberhard Feess, Natalie Packham                      | <i>Incentive Schemes, Private Information and the Double-Edged Role of Competition for Agents</i>   |
| 474 | Steven Ongena, Ibolya Schindele, Dzsamila Vonnák                        | <i>In Lands of Foreign Currency Credit, Bank Lending Channels Run Through?</i>  |
| 473 | Fabian Kindermann, Dirk Krueger   | <i>High Marginal Tax Rates on the Top 1%?</i>   |
| 472 | Gianmarco Ottaviano, João Paulo Pessoa, Thomas Sampson, John Van Reenen | <i>The Costs and Benefits of Leaving the EU</i>   |
| 471 | Dimitris Christelis, Dimitris Georgarakos, Tullio Jappelli              | <i>Wealth Shocks, Unemployment Shocks and Consumption in the Wake of the Great Recession</i>  |